International Space Science Institute, 15-19 October 2012, Bern, Switzerland

Power-law distributions of Flare Brightenings and Fractal Reconnection in a solar flare

Naoto Nishizuka (ISAS/JAXA)

and Kazunari Shibata
(Kwasan and Hida obs. Kyoto University)

Nishizuka et al. 2009, ApJL, "The Power-law Distribution of flare kernels and Fractal current sheets in a solar flare" + Nishizuka & Shibata submitted to PRL

Multi-wavelength emission in a Solar Flare

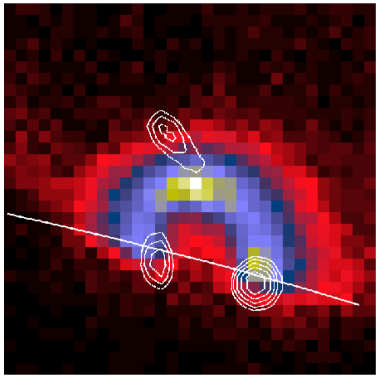

Impulsive flares
(Masuda 1994)

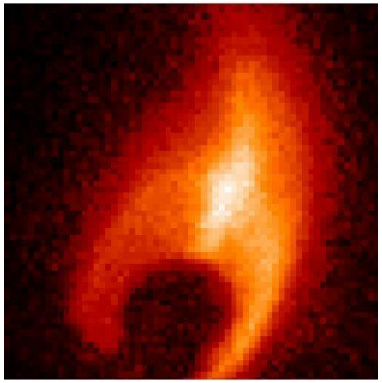

LDE flares
(Tsuneta 1992)

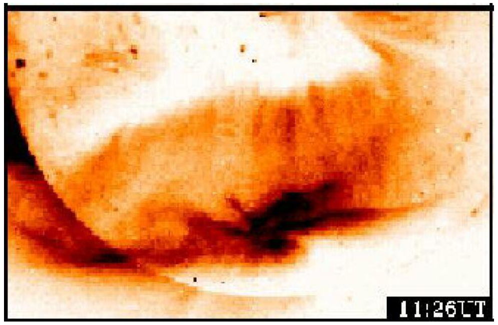

Giant arcades (CMEs)
(McAllister)

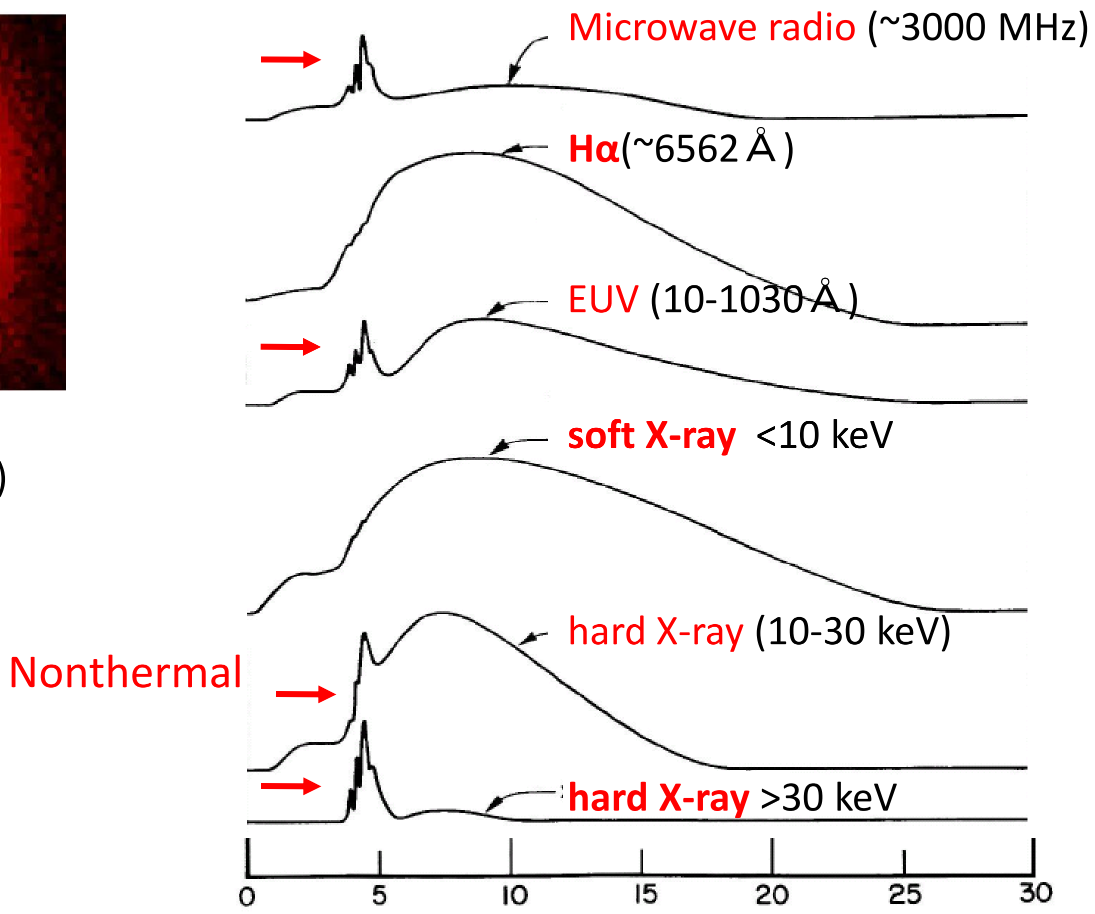

(Kane 1974)

Multi-wavelength emission in a Solar Flare

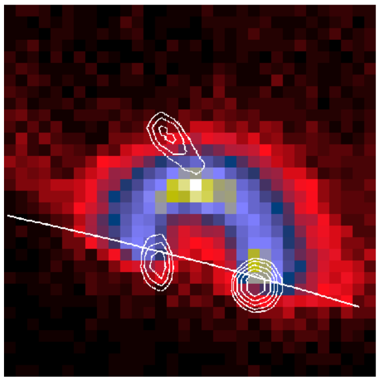

Loop-top HXR source
（Masuda 1994)

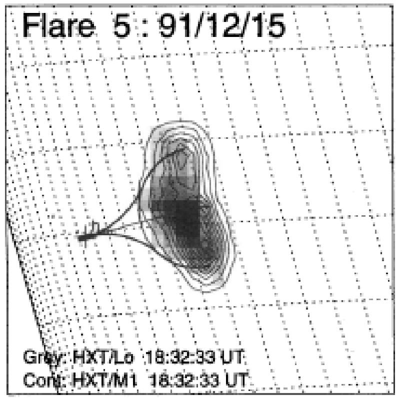

Time-of-flight method
[Aschwanden 1996]

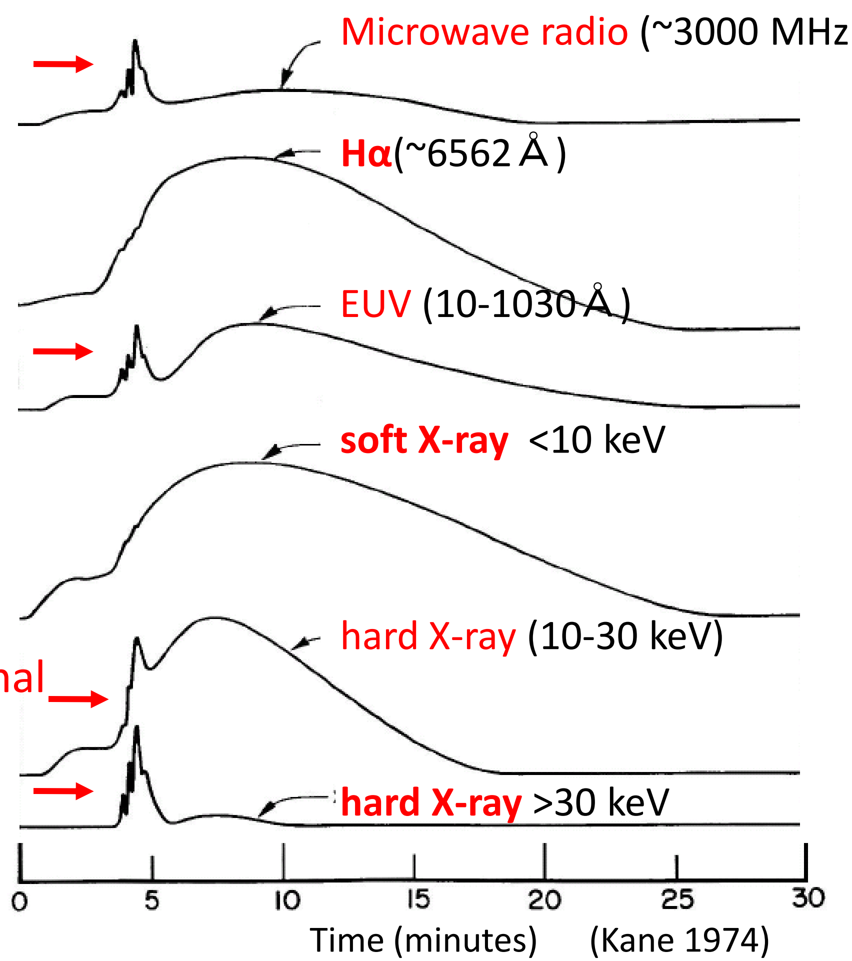

- Particle acceleration region is above the soft HXR loop (loop-top HXR source or higher corona)
- Acceleration occurs in a small region ~1000km (Non-thermal pulse ~10-100ms)
- How about 3D structure of acceleration region? [Global model of particle acceleration in a flare]

Plasmoid (flux rope) ejection

(Yohkoh and Hinode observations)

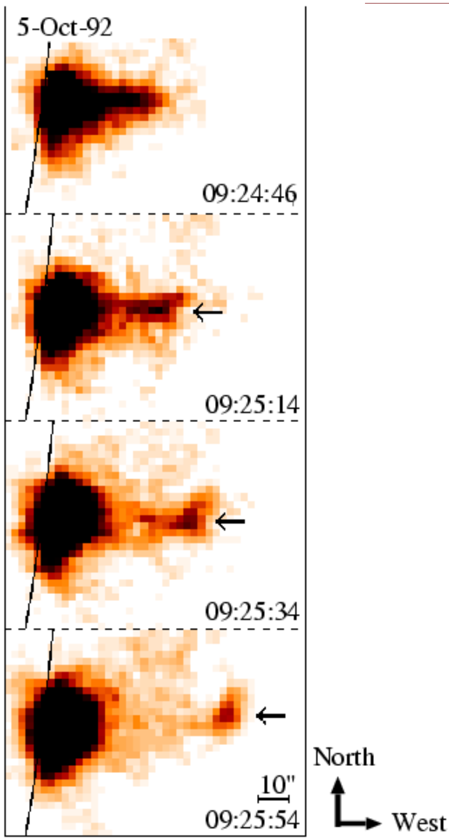

impulsive flares
~ 10^9 cm

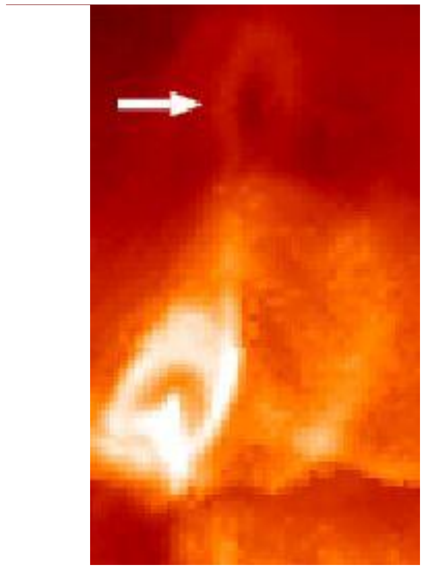

E(Long Duration
ent) flares
0^10 cm

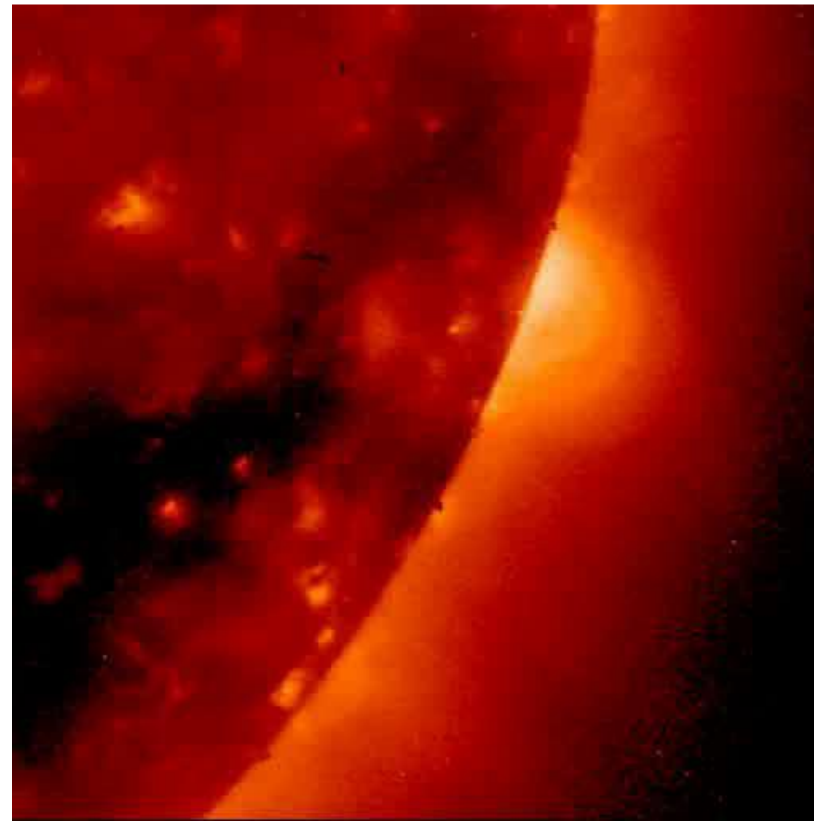

2008 Apr 9 Hinode / XRT

Plasmoid (flux rope) ejection

(Yohkoh and Hinode observations)

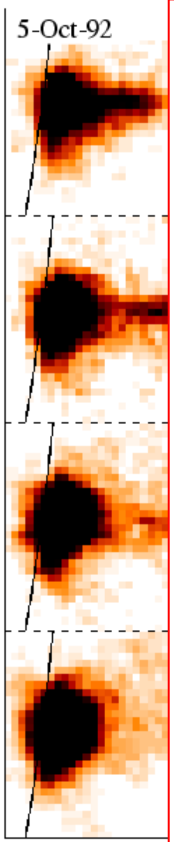

impuls
~ 10^

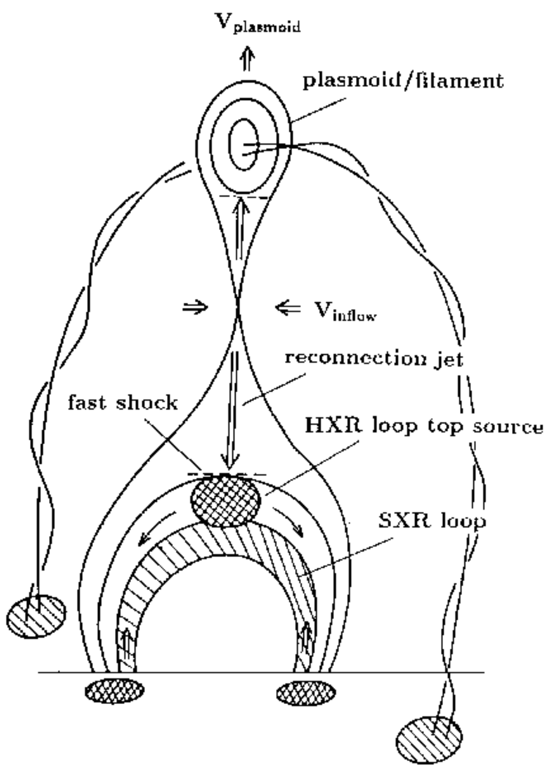

Plasmoid-Induced
-Reconnection model
(Shibata 1999)

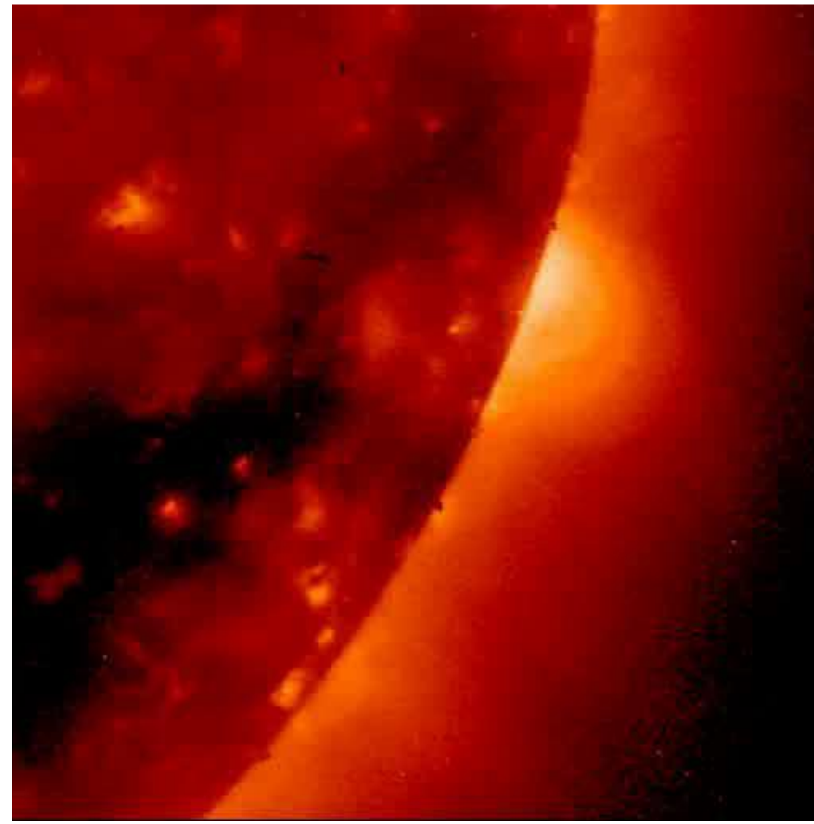

2008 Apr 9 Hinode / XRT

Fractal behavior of hard X-ray/ microwave bursts and energy release mechanism

- Intermittent Hard X-ray burst, radio/microwave burst

(e.g. Frost, Dennis, Kane, Kiplinger, Benz, Aschwanden, Kliem, Karlicky)

fragmented Current Sheet

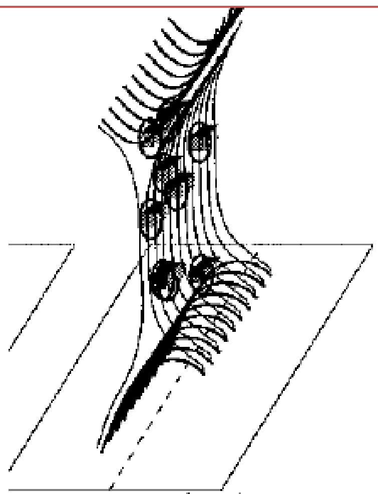

[Aschwanden.2002]

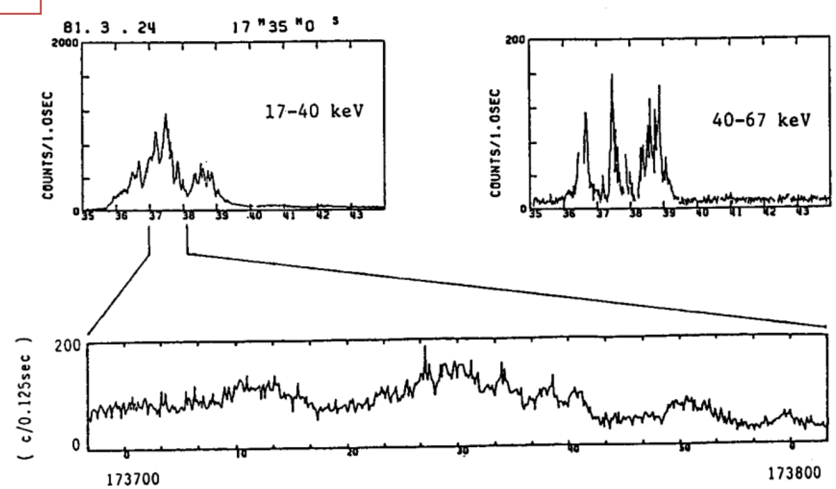

[Ohki et al..1992]

Fractal Current Sheet

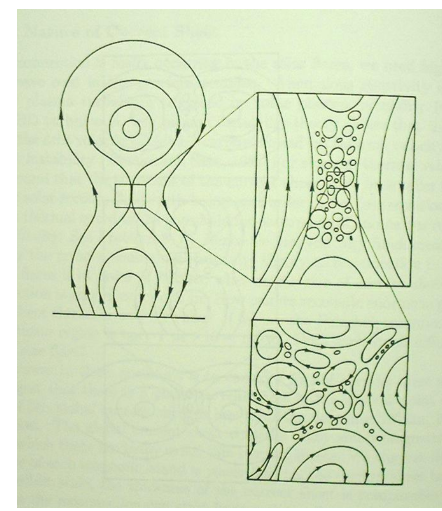

[Tajima & Shibata 1997]

Observation of hard X-rays and microwave emissions show fractal-like time variability, which may be a result of fractal reconnection and associated particle acceleration.

3D Energy Release in a Solar Flare (multiple downflows by patch reconnection)

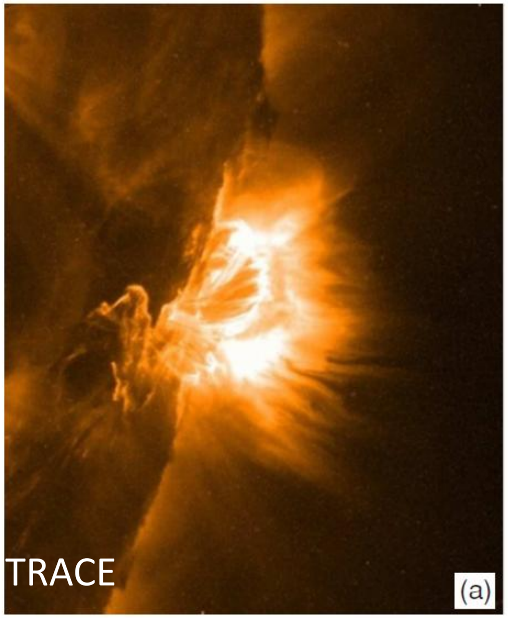

Multiple-downflow

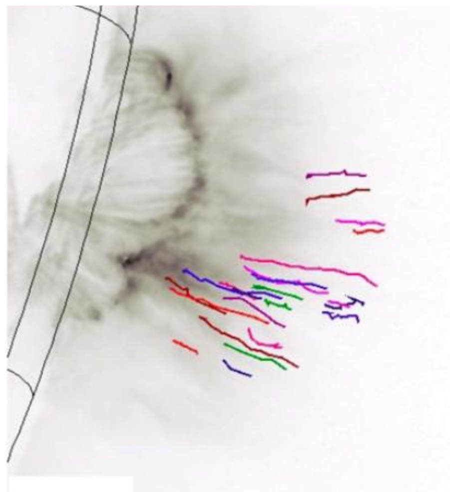

2002 April 21 flare [McKenzie & Savage 2009]

Area of the downflow region

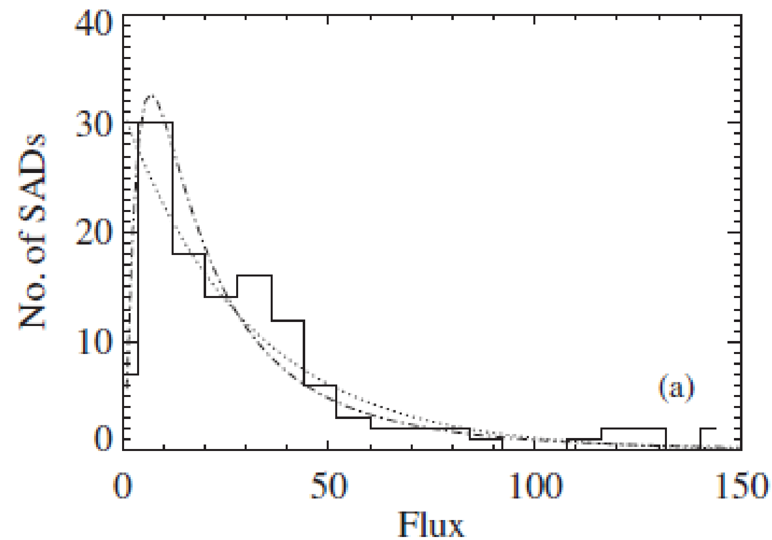

[McKenzie & Savage 2011]

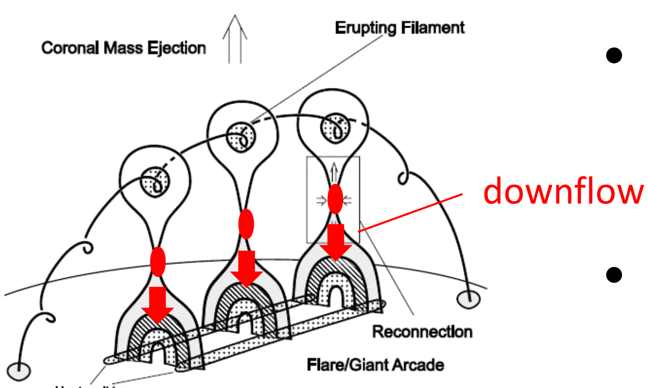

- Energy release (patchy reconnection) intermittently occur in a solar flare along the neutral line.
- Multiple downflows show log-normal distribution in the area and magnetic flux.

Remaining Puzzles in Flares/CMEs

- Where and How do Reconnection and Particle acceleration occur in Flares/CMEs?
- What determines the reconnection rate and the energy release rate?
- Scale gap between micro and macro-scale physics.
  -- microscale 1-100 cm, macroscale 10^8-10^{10} cm
- Avalanche of many small-scale events can explain the global-scale dynamics of CME/flares?
  --power-law and log-normal
- What's the role of a Plasmoid/Flux rope ejection?
  --contribution to Reconnection rate, Energy release rate, and particle acceleration process.

Scenario of fast reconnection
(Shibata and Tanuma 2001)

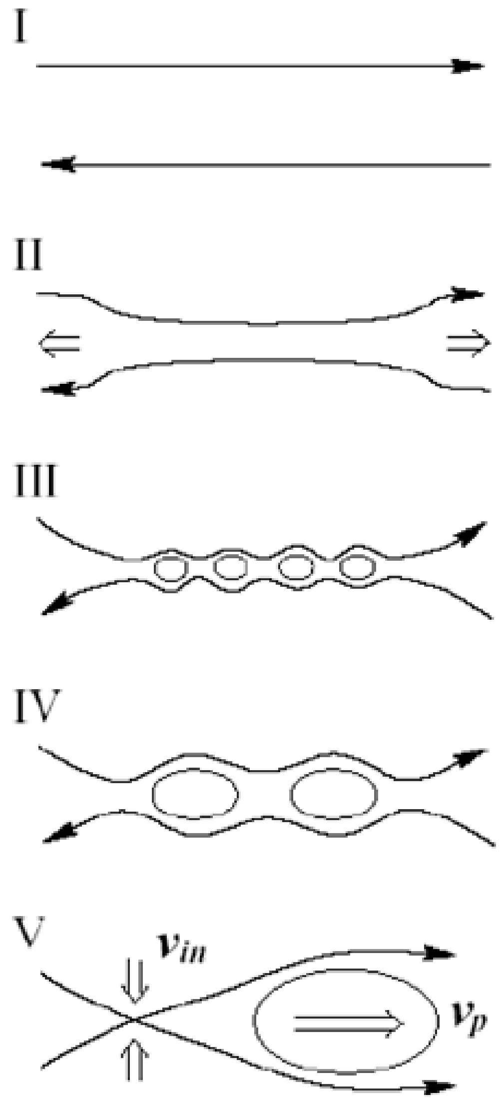

Cf) Hoshino et al. 1994
Lee-Fu 1986
Kitabata, Hayashi, Sato 1995

(1) Tearing instability

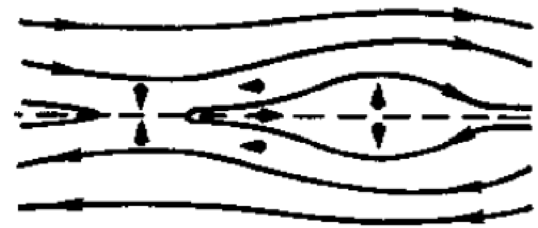

[Furth et al. 1963]

(2) Coalescence instability
(merging/inverse cascade)

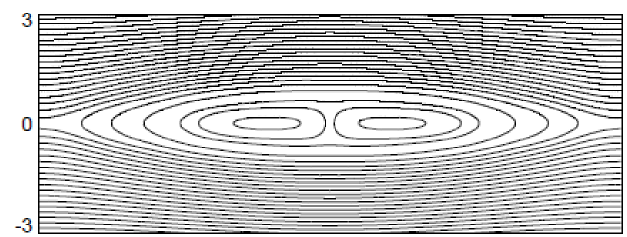

[Schumacher and Kliem 1997]

What is the Role of Plasmoid Ejections ?

(Shibata-Tanuma 2001)

(1) To store energy by inhibiting reconnection

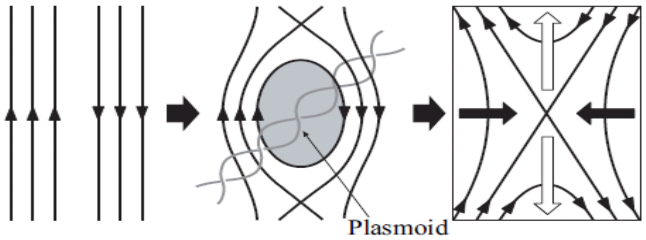

larger plasmoid

↓

larger energy release

(2) To induce strong inflow into reconnection region

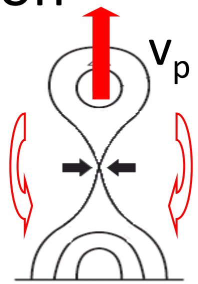

$$v_{in} = \frac{w_p}{L_{in}} v_p$$

reconnection ⇒ Plasmoid ejection ⇒ Strong inflow ⇒ reconnection

Ohyama-Shibata 1997, 1998 ⇒ Nonlinear Instability

cf. Ugai

Pile Up

↓

Reconnection (or external force i.e. disturbance)

↓

Avalanching of plasmoid ejections

Multiple plasmoids in a Current Sheet

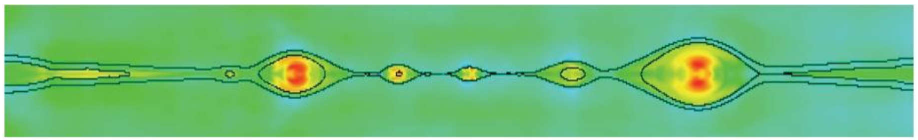

[Loureiro et al. 2009]

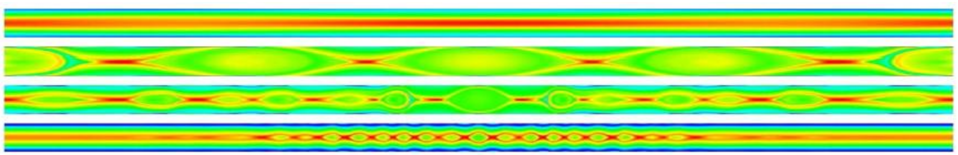

[Samtaney et al. 2009]

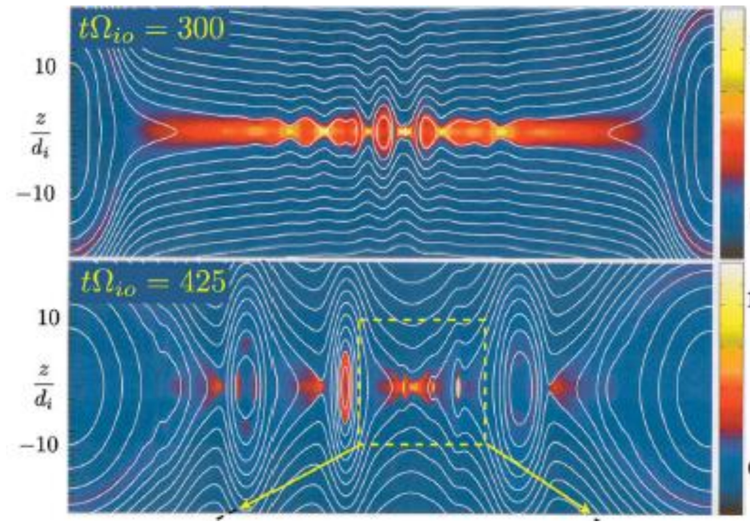

[Daughton et al. 2009]

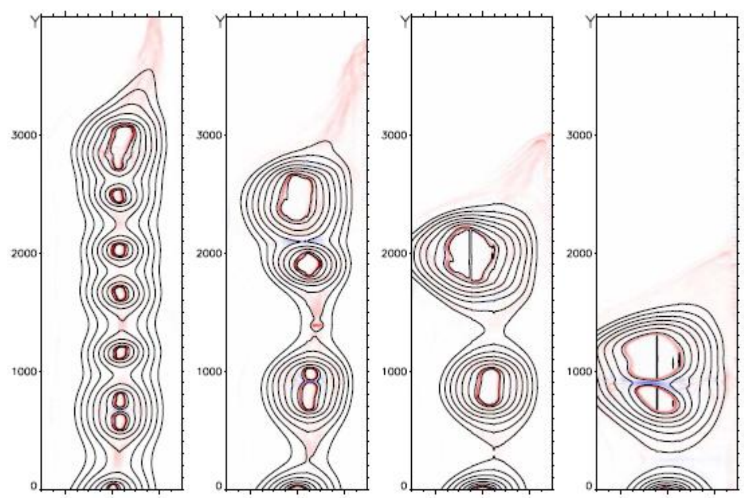

[Karlicky and Barta. 2011] **Friday Talk**

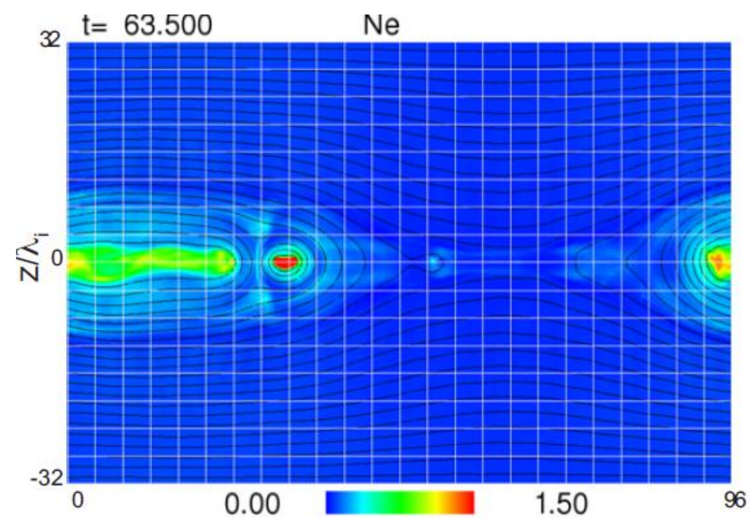

[Tanaka et al. 2010]

Multiple plasmoids in a

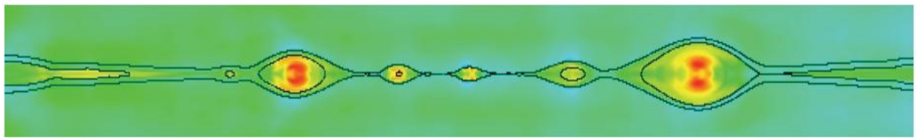

[Loureiro et al. 2009]

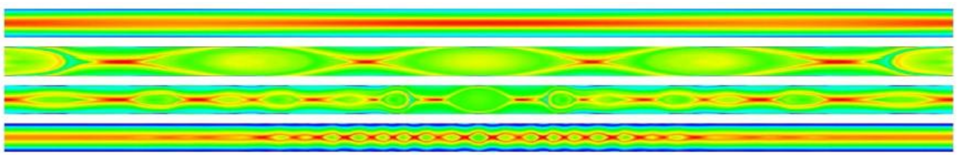

[Samtaney et al. 2009]

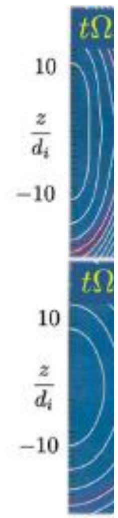

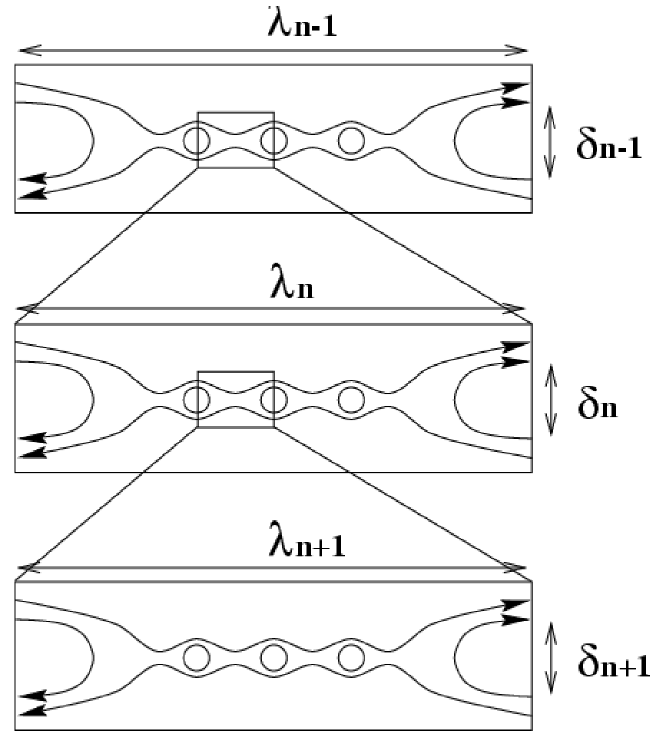

[Shibata and Tanuma 2001]

Fractal Reconnection

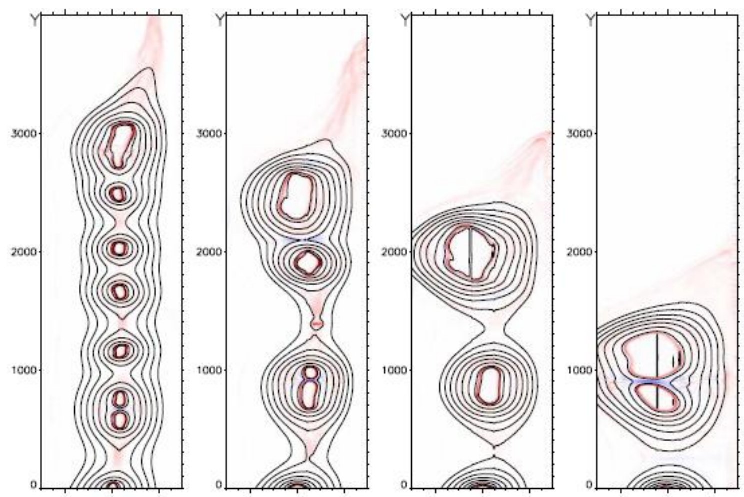

[Karlicky and Barta. 2011] **Friday Talk**

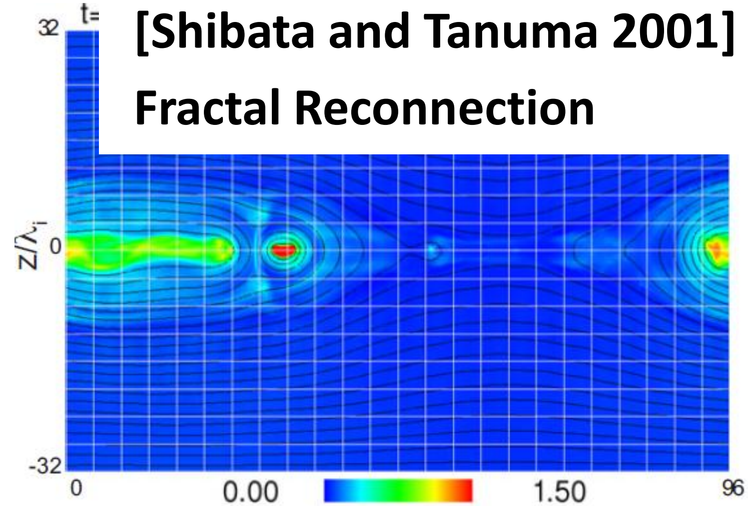

[Tanaka et al. 2010]

2D Fractal Current Sheet and Affect on Magnetic Reconnection Rate

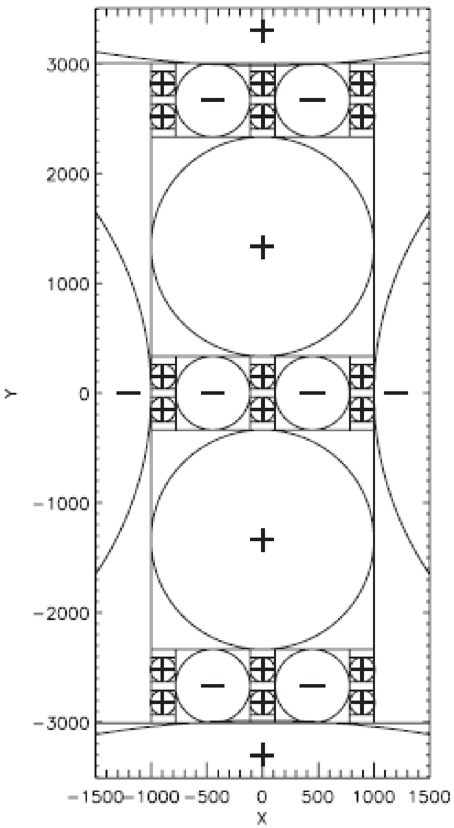

Figure 9. Example of the fractal reconnection structure corresponding to relations (2) and (3), for $A = 2$ and $B = 3$. Double straight lines delineate current sheets with interacting plasmoids (circles). The plus and minus signs express the orientation of electric currents in the plasmoids. X and Y are in arbitrary units.

[Karlicky 2011 ApJ]

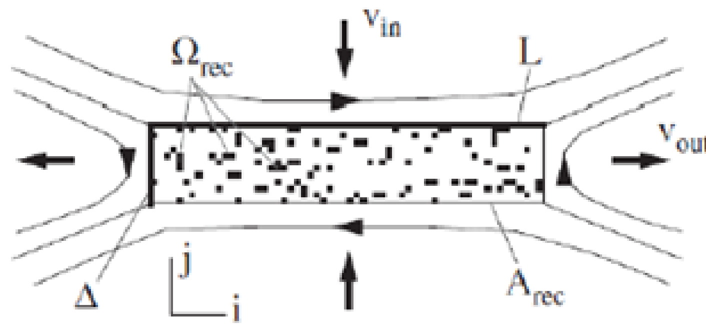

$$\mathcal{M}_{\mathrm{FRM}}(\mathcal{R}_m; D) = \mathcal{R}_m^{-(D/D+1)}.$$

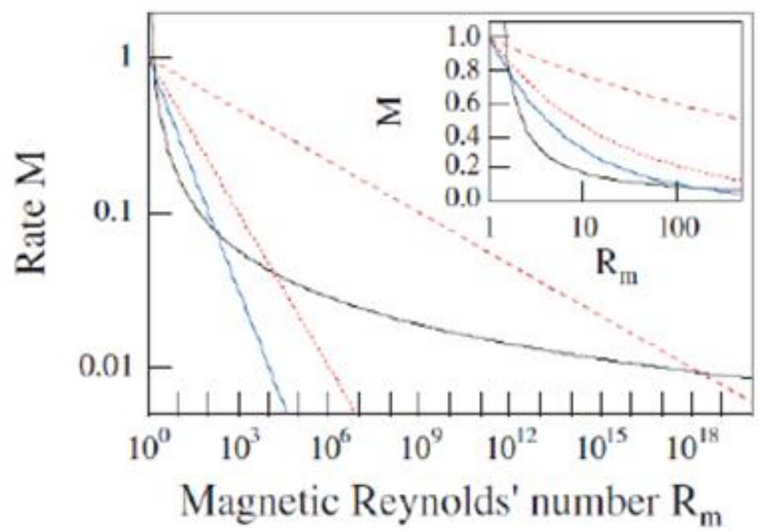

-Sweet-Parker model

-Petchek-like model

▪ ▪ ▪ (dotted) D=1/2

-----(dashed) D=1/8

Fractal dimension

[Materassi, Consolini 2007 PRL]

cf) Turbulent Reconnection [Lazarian&Vshniac 1999]

Multiple Plasmoid ejections

Yohkoh/SXT [Nishizuka et al. 2010]

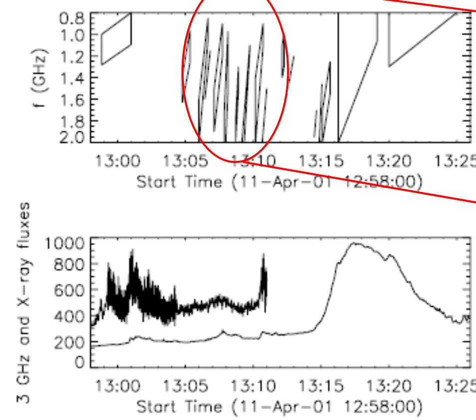

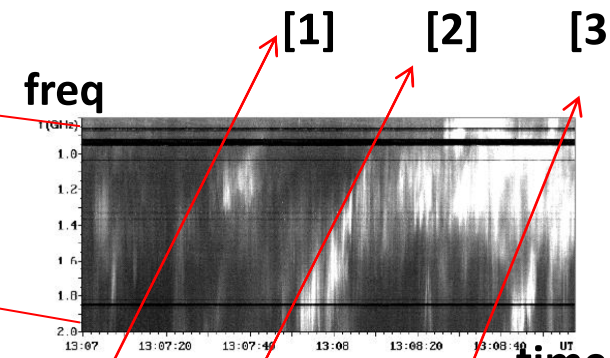

Fig. 3. Example of high-frequency slowly drifting structures observed by the Ondřejov radiospectrograph in April 11, 2001 at 13:07–13:09 UT.

Slowly drifting radio source (Karlicky et al. 2004 AA)

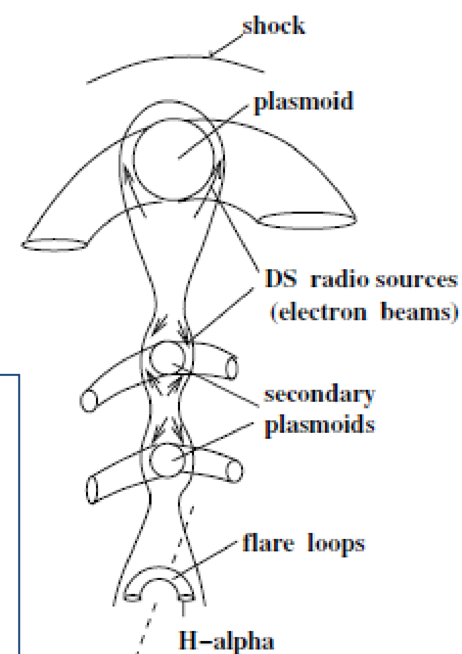

Signature of small scale secondary plasmoid ejections ?

(Kliem et al. 2000, Shibata and Tanuma 2001)

Particle acceleration associated with Multiple plasmoid ejections and Downflows

- Plasmoid ejection associated with hard X-ray burst : [Nishizuka et al. 2010]
- Downflow associated with hard X-ray burst: [Asai et al. 2003]

Time slice image (**plasmoid ejection**)

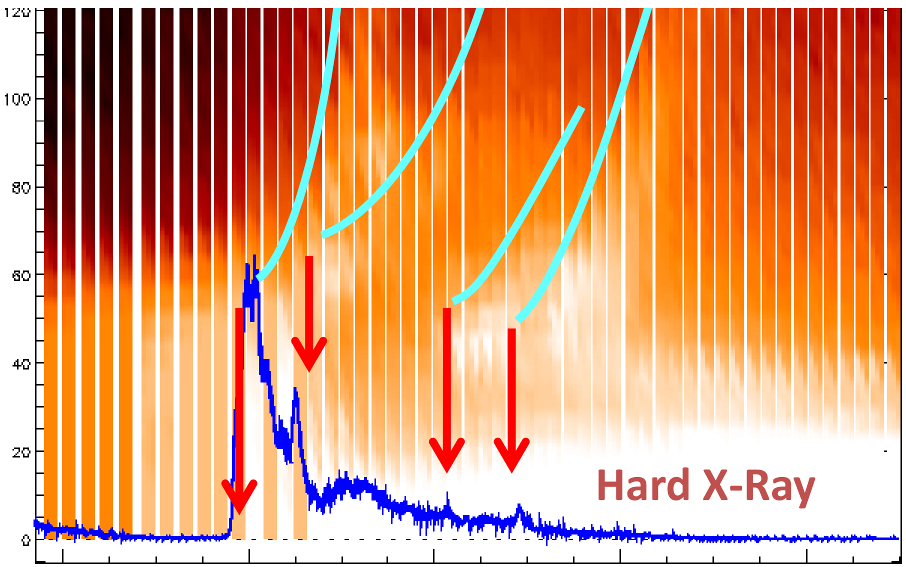

Time slice image (**downflow**)

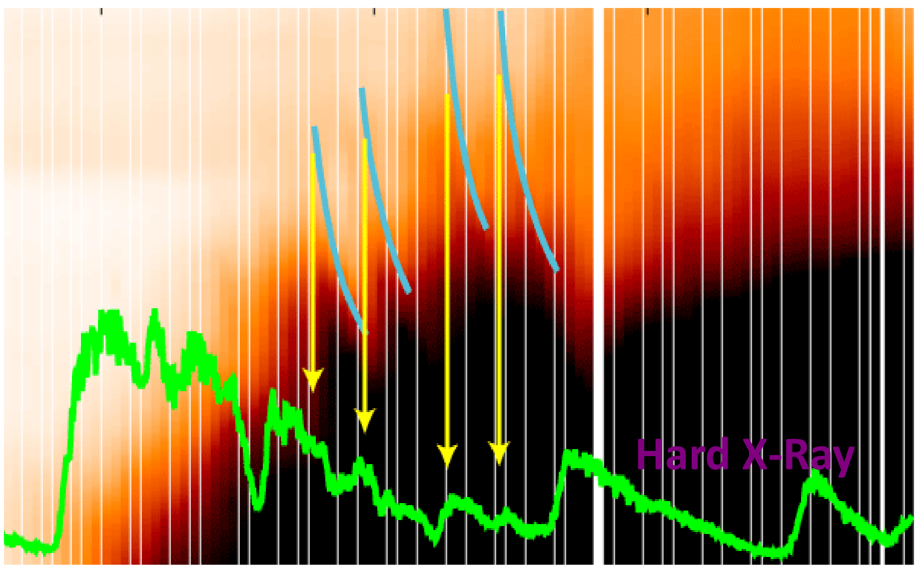

These observations may indicate that particle acceleration is related to plasmoid ejections and downflows in a turbulent (fractal-like) current sheet.

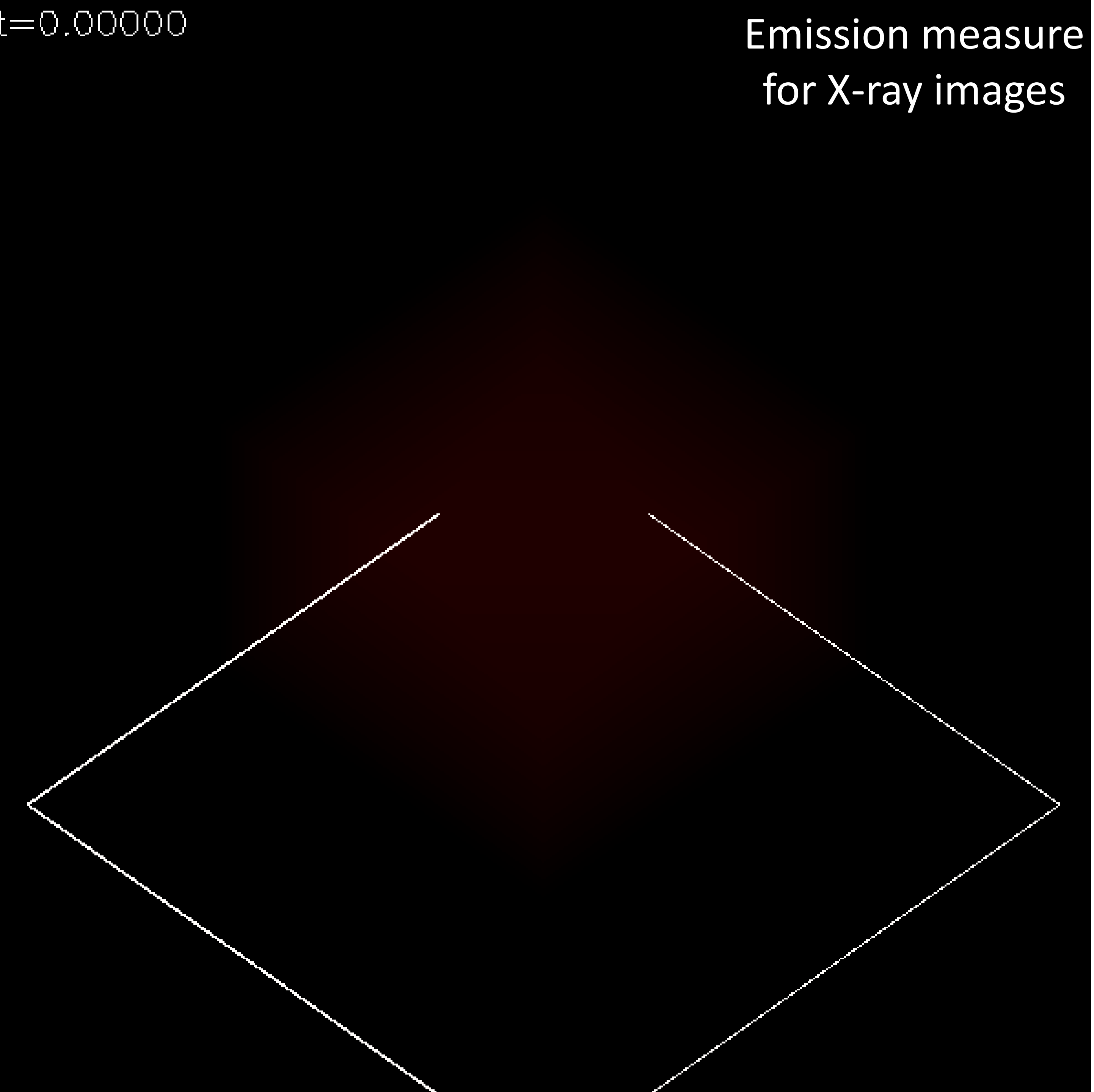

Nishida, Nishizuka, Shibata, submitted APJL

density

temperature

Turbulent structure in 3D current sheet

Nishida, Nishizuka, Shibata, submitted APJL

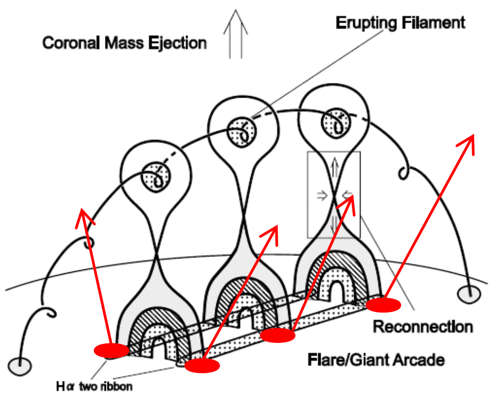

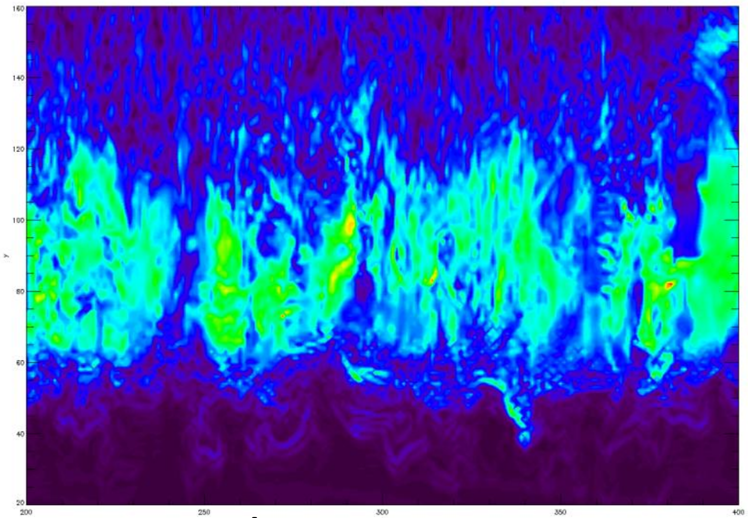

Current density

Velocity Vz

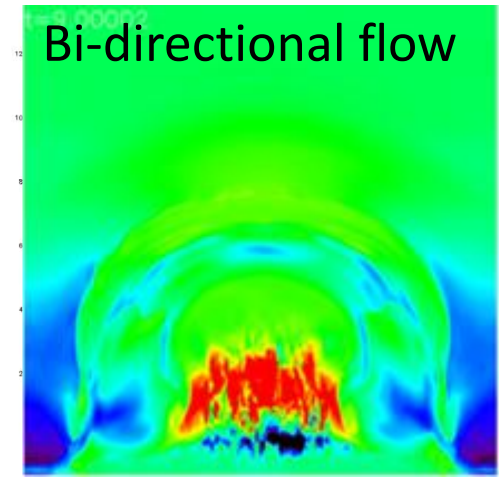

Current density

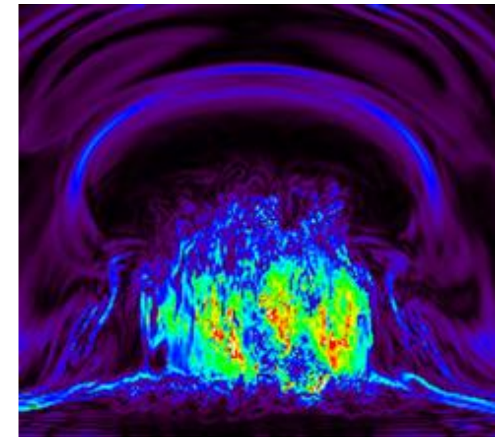

- 3D reconnection forms turbulent fractal structure in a current sheet.
- Multiple plasmoid ejections enhance E-field, and particle acceleration occurs intermittently. **This should be observed as a fractal-like behavior of flare kernels at the footpoints of the loops.**

Motivation of this study

- Where and How do Reconnection and Particle acceleration occur in Flares/CMEs?

--What is the 3D configuration of a current sheet?

--Sweet-Parker current sheet? or there exists a Turbulent or Fractal current sheet with multiple plasmoids in the corona?

Indirect observation of a current sheet,
from the **footpoint brightenings (flare kernels)**
of a solar flare.

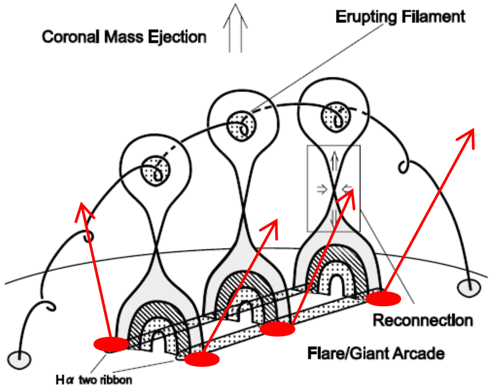

Multi-wavelength Observation

X2.5 class on 2004 November 10: onset 2:00UT peak 2:15UT

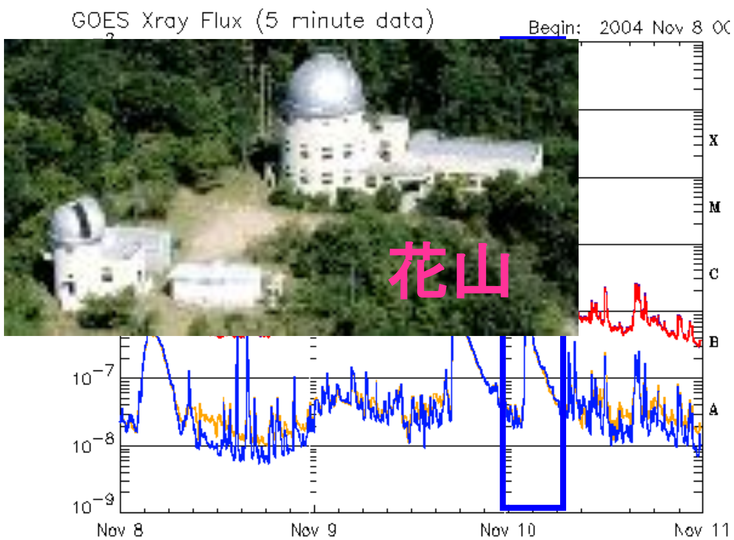

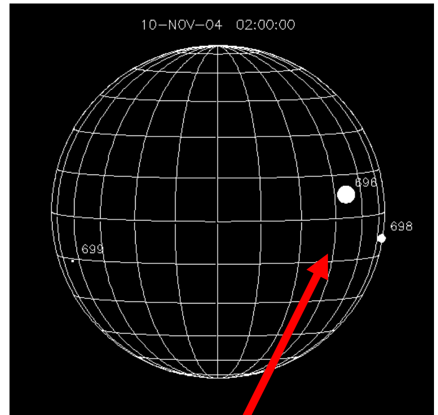

(720”,100”)

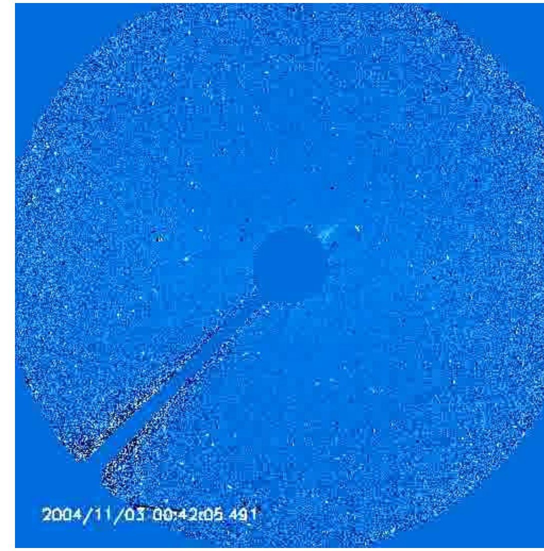

Obs. Satellite / data name	Temporal res.	Spatial res.
TRACE :1600A (C IV 1550A), white light	3-4s	1”
Sartorius(Kwasan obs.):Hα(6562Å,wing+1.0Å)	1-3s	(1”)
SOHO : MDI, white light	90min	2”
RHESSI : HXR > 25keV	> 4.0s	2”

Advantage：Obs. with High temporal/spatial resolution in Flare mode

2004 November 10
X2.5-class Flare

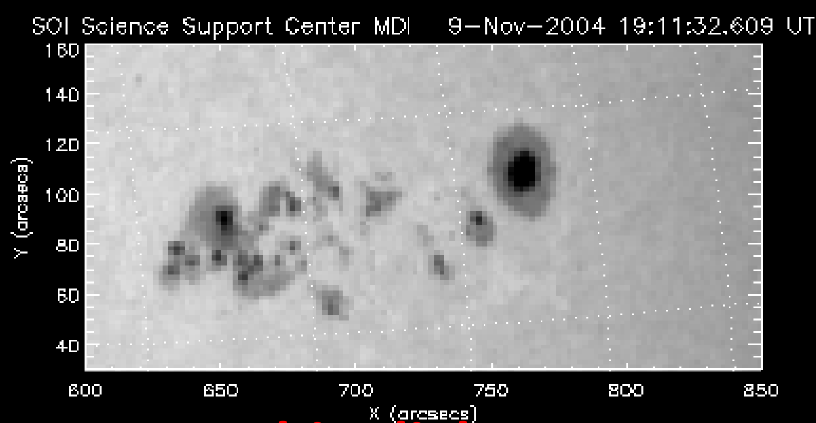

TRACE white light

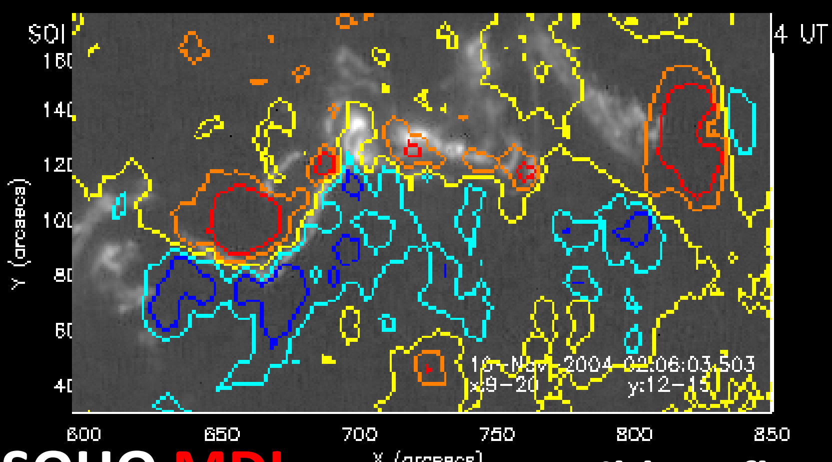

SOHO MDI **+ C IV two ribbon flare**

500G 250G 0G -250G -500G

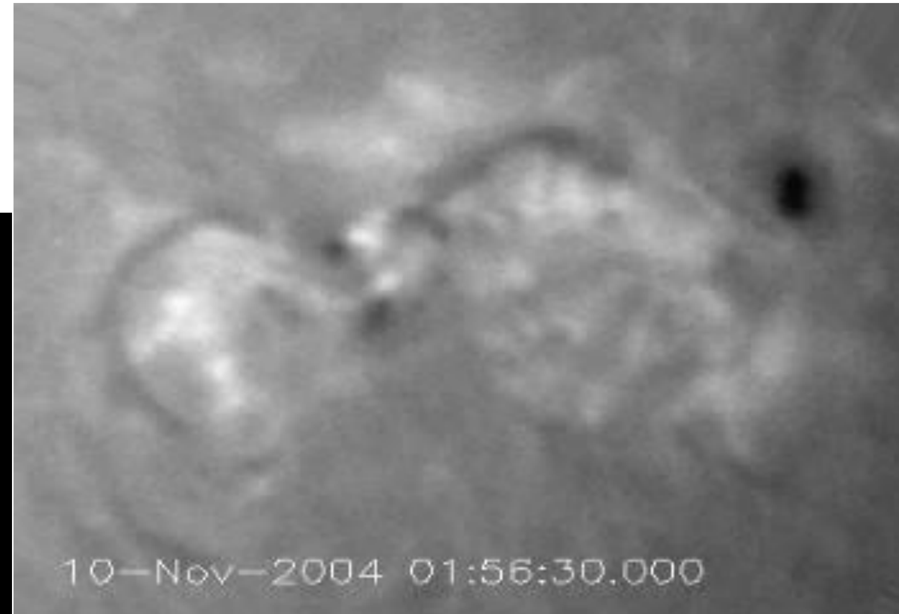

Sartorius Hα image

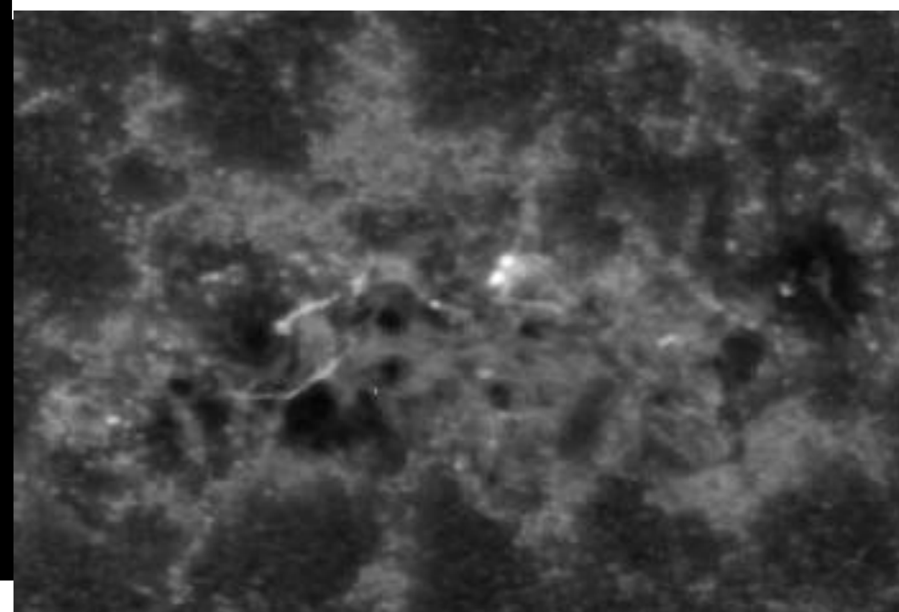

TRACE1600 Å (C IV image)

Hα and UV Filament eruption

Hα Filament eruption

UV filament erupt.

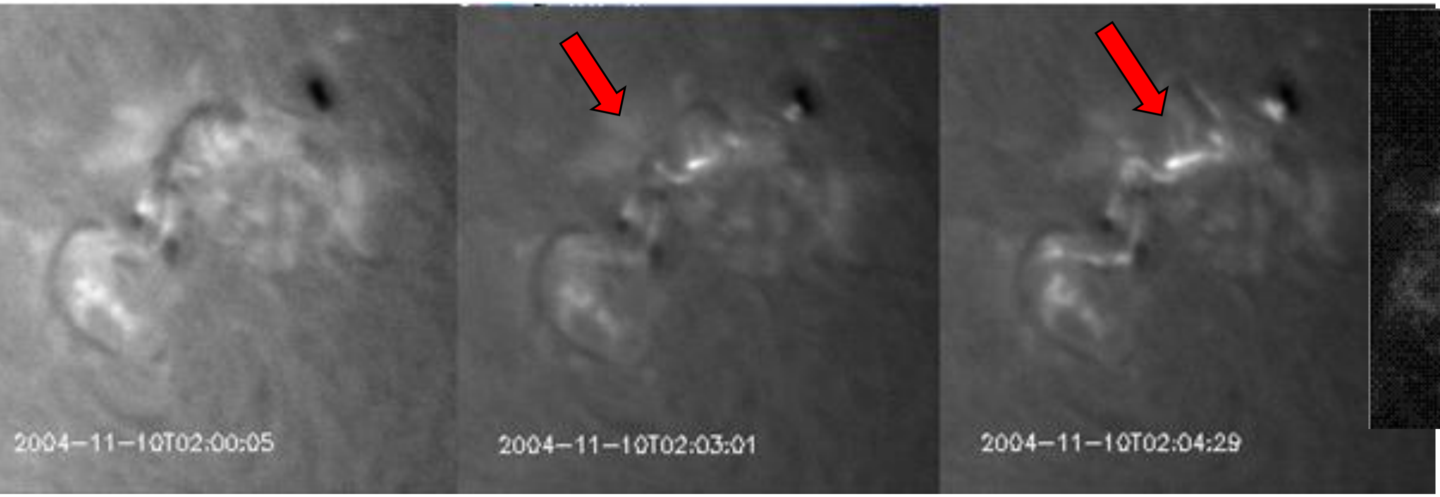

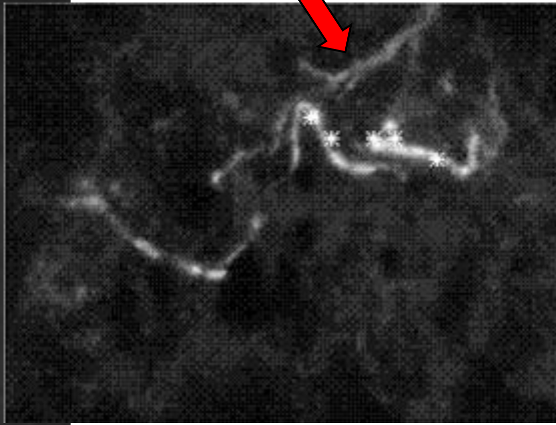

C iv (UV) image

Sartorius Hα image

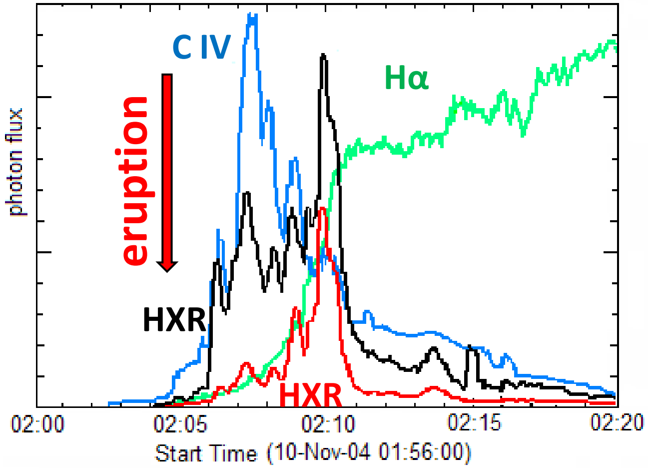

Hα・C IV・HXR(50-100keV)・ HXR(25-50keV)

- **Hα filament** (~10^4 K) is ejected at the beginning of the flare, and **brightening starts just below the eruption**.
- The filament eruption was also observed in UV emission (T~10^5 K).

Filament eruption triggers Impulsive reconnection.

Time variations of HXR/C IV Flare kernels

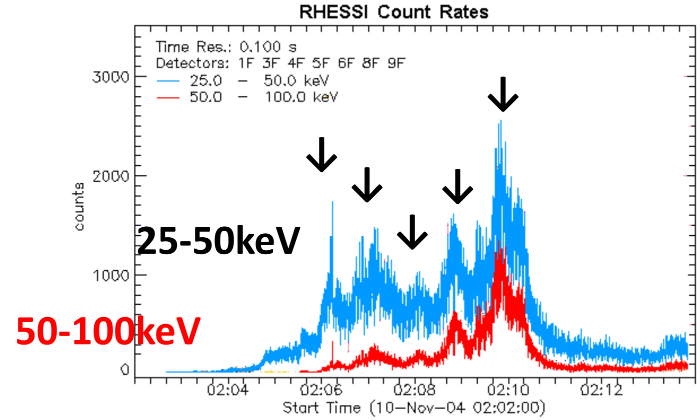

■ **Distribution of HXR sources (white), with C iv flare ribbon (back ground image)**

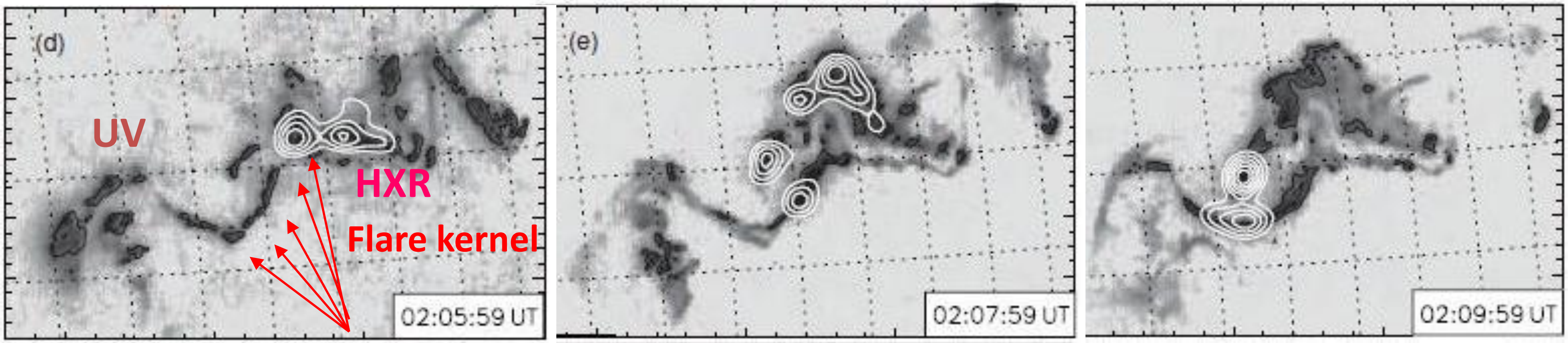

■ **Distribution of C IV flare kernels (I >500 counts)**

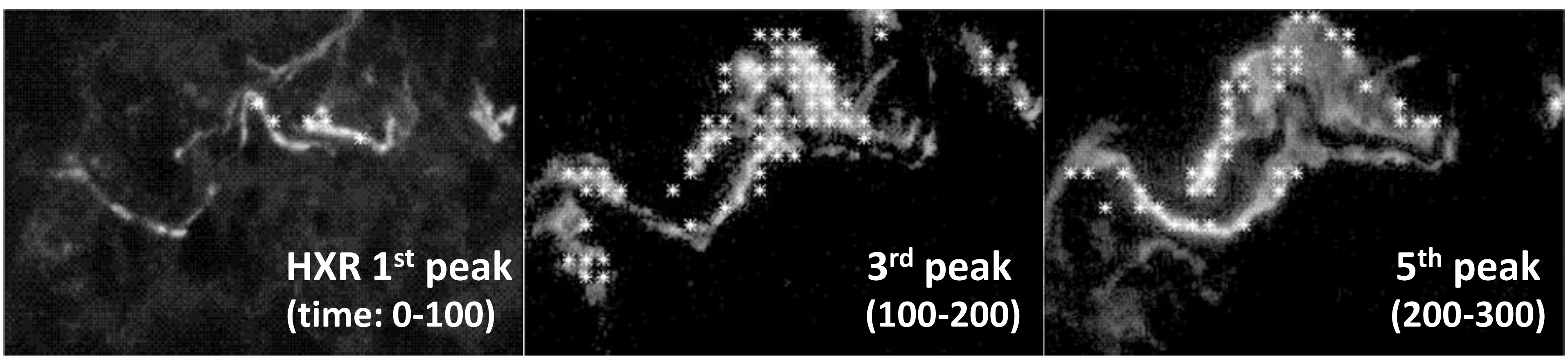

Spatial and Temporal Correlation among HXR, Hα and UV flare kernels/ribbons.

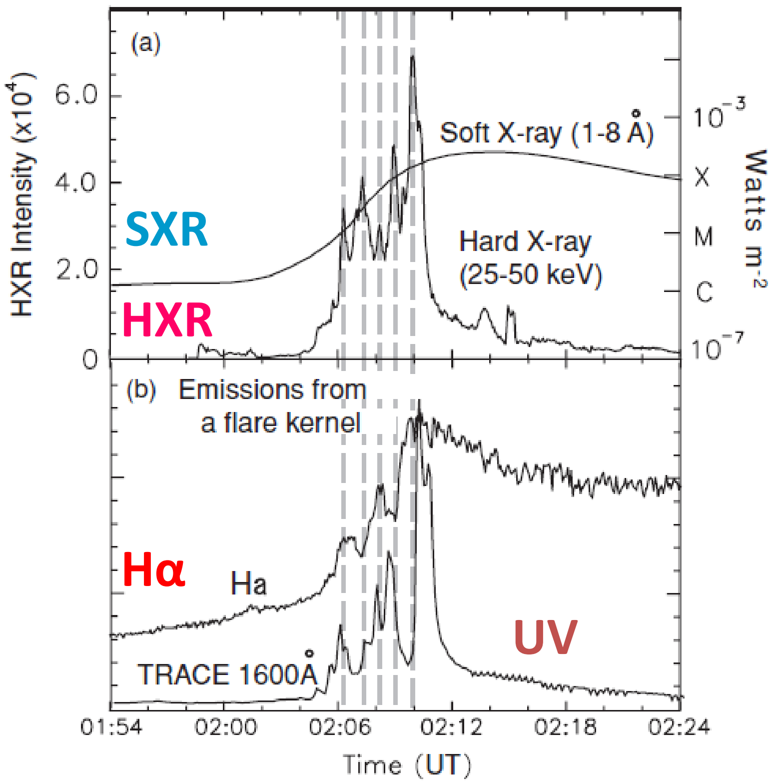

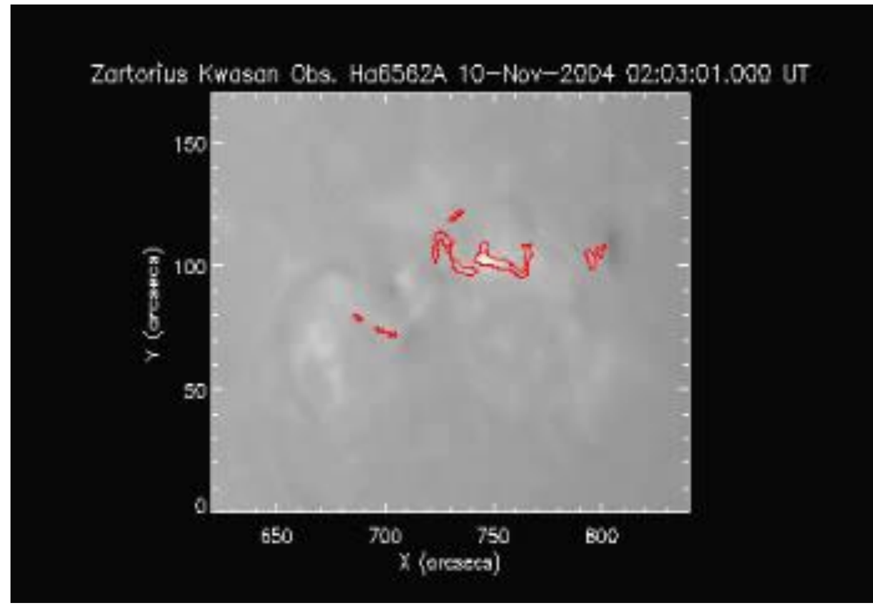

↑Hα two ribbon + C IV contour

C IV flare kernels are cased by the same physical process as HXR ・Hα (nonthermal particles)

- The positions/timing of C IV・Hα・HXR kernels are well correlated.
- The outer ridge of two ribbon of C IV and Hα is (inside not)well fitted

Measurement of Footpoint kernels

Information of foot point kernel

(intensity /timing / duration /position) ⇒ (I_{peak}, t_{peak}, t_{dur}, x)

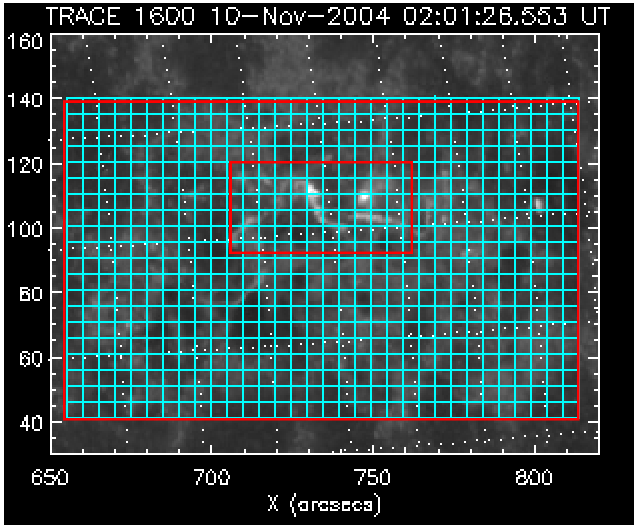

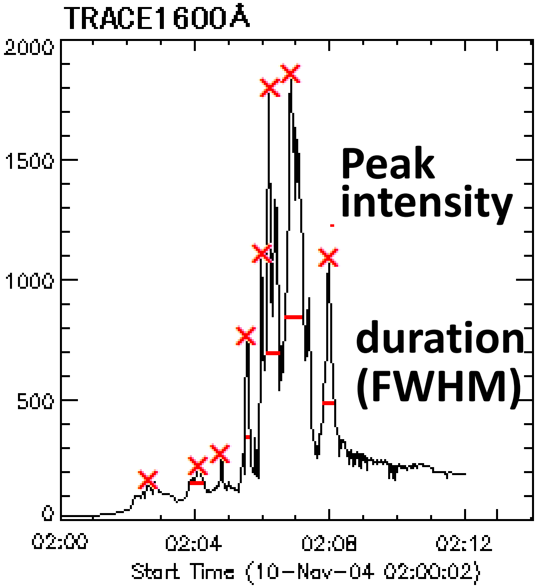

*Intensity
⇔ Energy of a plasmoid

*Duration
⇔ Size of a plasmoid

Data:TRACE1600 Å (Assuming this as C IV line in impulsive phase)

①To Draw averaged time profiles over meshes separated with 5arcsec

②To Record peak intensities / timings/ durations of each time profiles

Sampling number ~ 700 ⇒ the same with 2arcsec mesh･･･

Time variations of Flare kernels

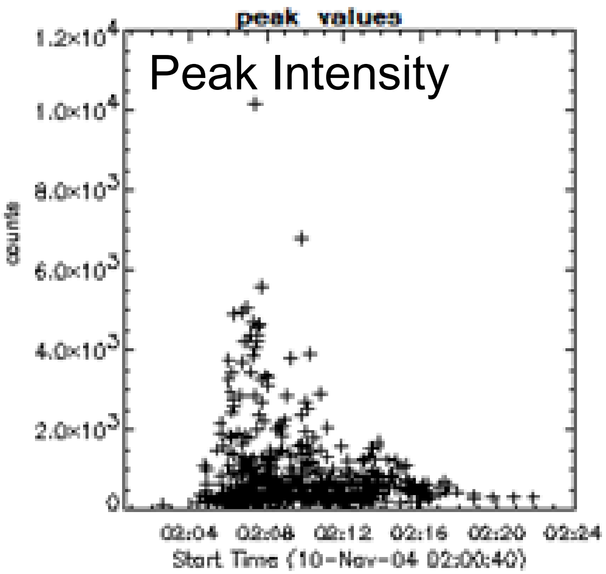

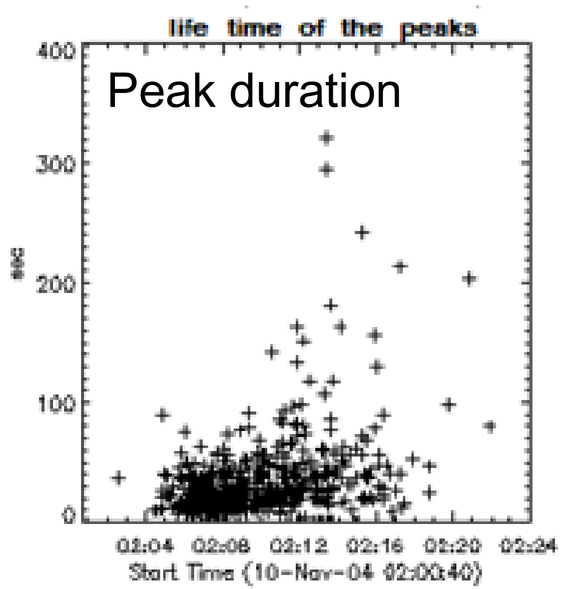

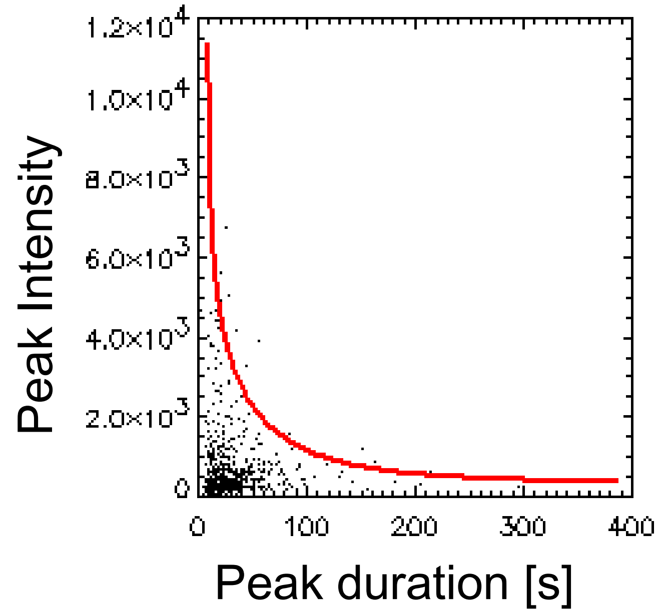

The property of flare kernels varies in time:

- **high intensity**, **short** duration (**Impulsive** phase)
- **low intensity**, **long** duration (**Decay** phase)

Distribution of flare kernels (Intensity･Duration)

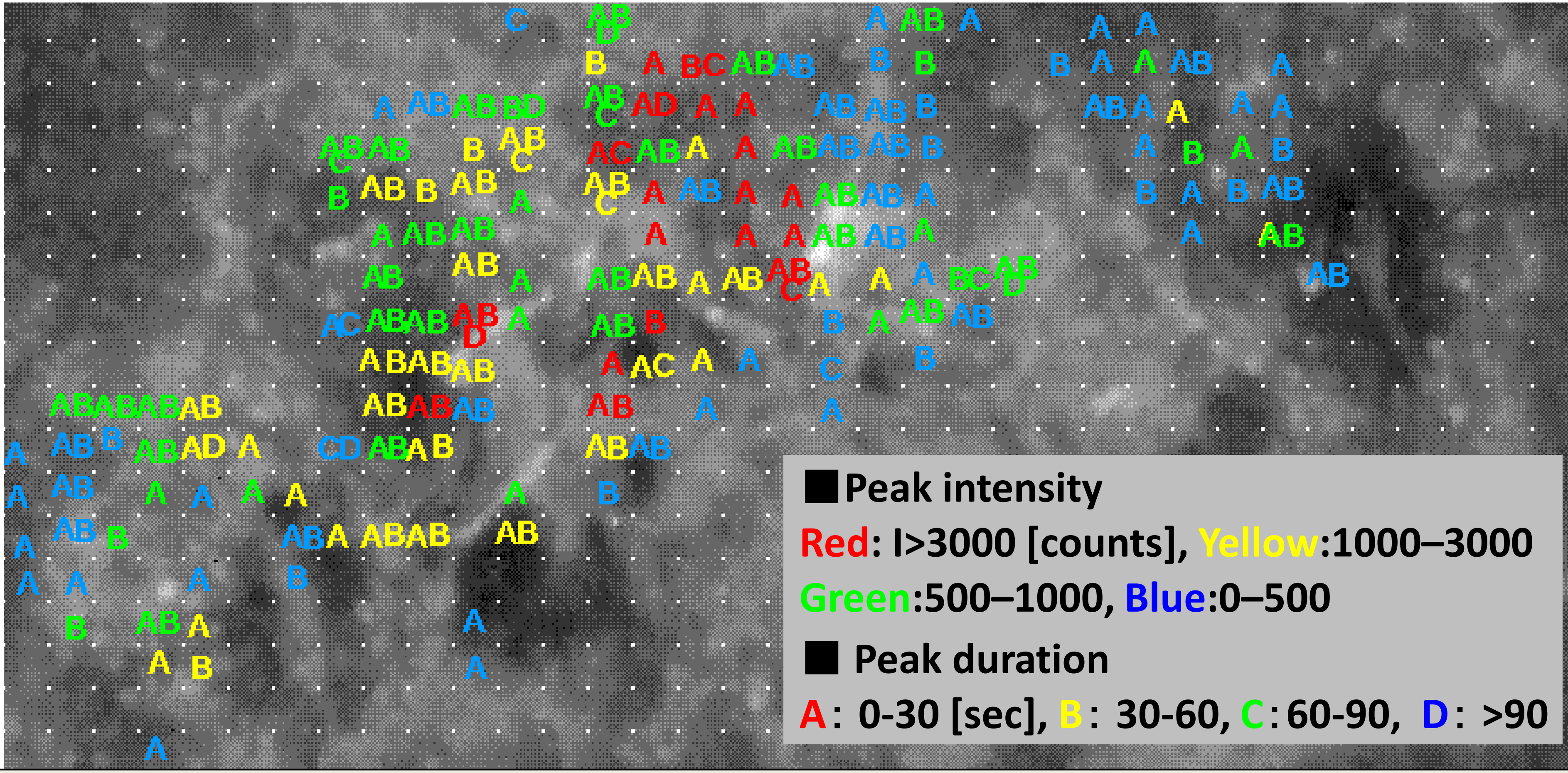

Flare kernels are **non-uniform**ly distributed:

- **High intensity** & **short** duration (**impulsive** phase, **near** the **neutral line**),
- **Low intensity** & **long** duration (**decay** phase, apart from the neutral line).

The distribution of peak intensity & duration

■ **Statistics of foot point kernels : mesh size = 5” (Whole region)**

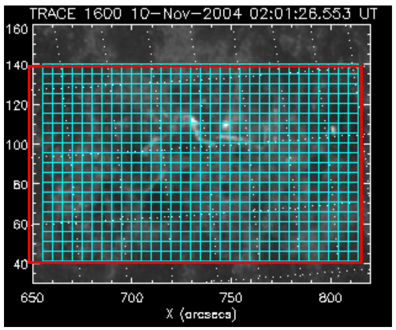

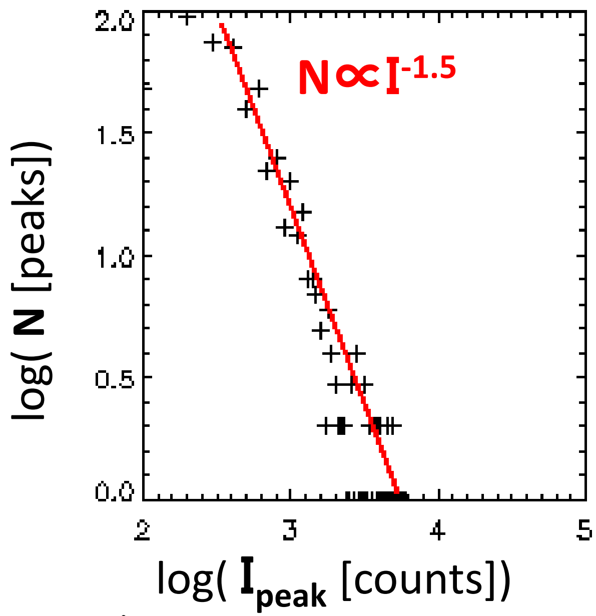

↑**distribution of peak intensity of kernels**

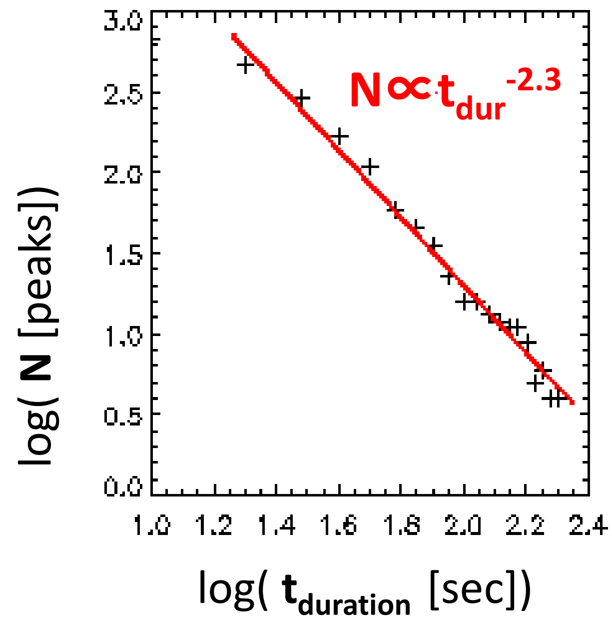

↑**distribution of peak duration of kernels**

→ **N∝I$^{-1.5}$**

→ **N∝$t_{dur}^{-2.3}$**

Peak intensity & duration of flare kernels in C IV image show power-law distribution in a single event.

The distribution of peak intensity & duration

■ **Statistics of foot point kernel : mesh size= 2” (limited area)**

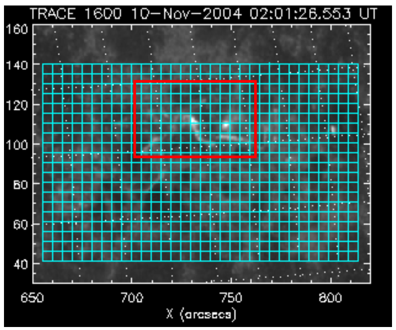

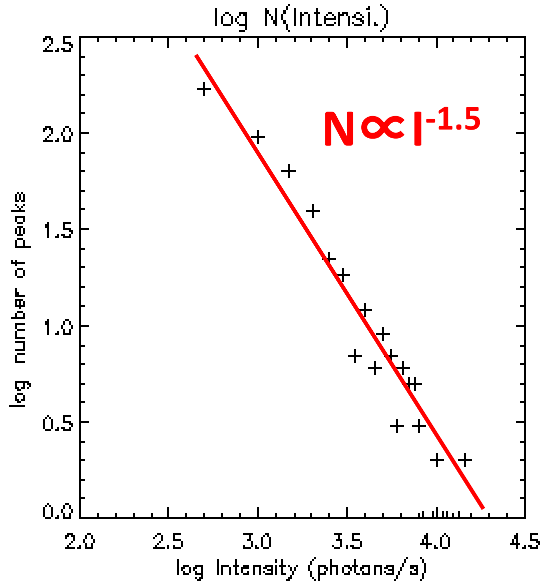

↑distribution of peak intensity of kernels

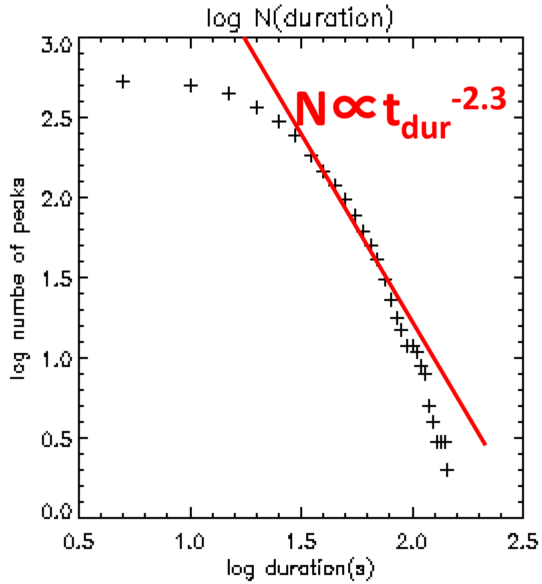

↑distribution of peak duration of kernels

- Peak intensity/duration/time interval follows power- law with 2” mesh

- Through the whole observation period, the distributions of flare kernels became power-law.

Results of Foot point kernel Analysis（2）

■Statistics of foot point kernel：mesh size= 2” (limited area)

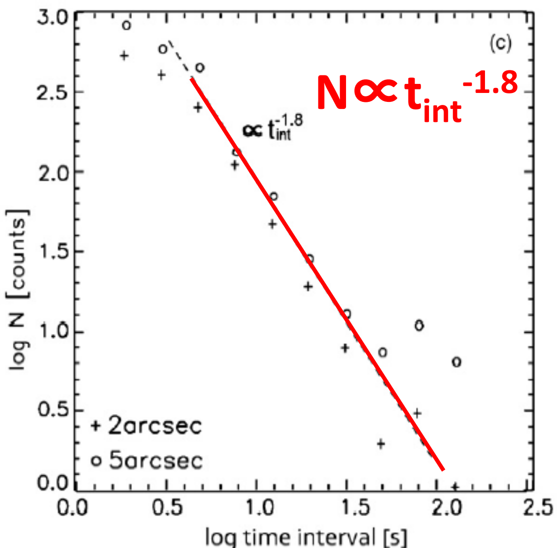

↑distribution of time Intervals of kernels

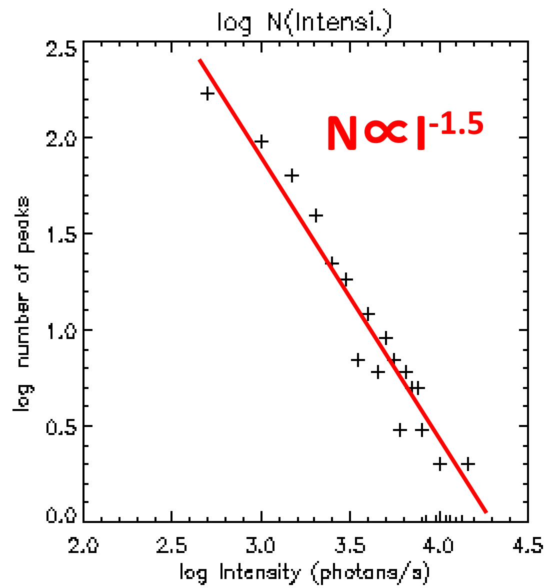

↑distribution of peak intensity of kernels

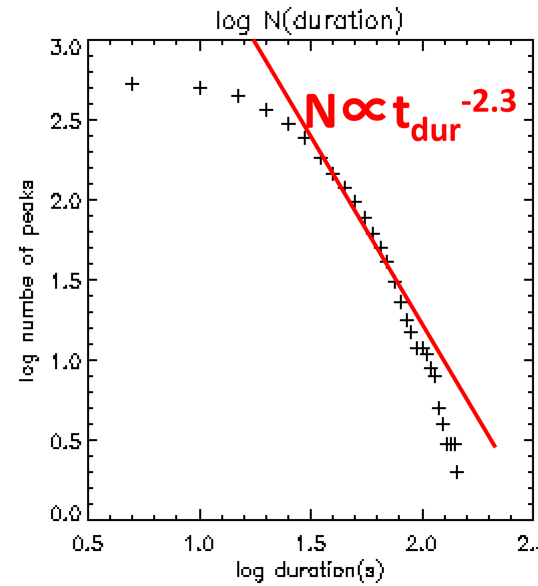

↑distrib durat

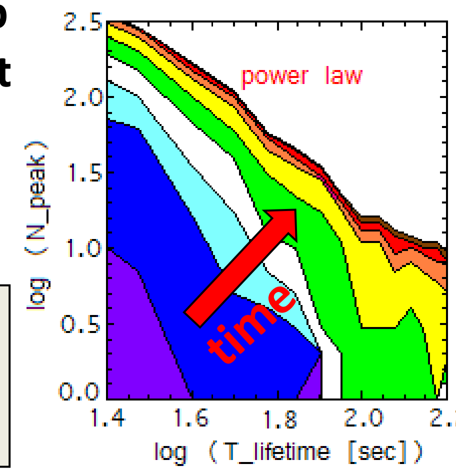

- Peak intensity/duration/time interval follows power- law with 2” mesh

- Through the whole observation period, the distributions of flare kernels became power-law.

Power-law distribution from a fragmentation structure in a solar flare (interpretation)

- **Peak intensity : $N \propto I^{-1.5}$**
- **Peak duration : $N \propto t_{dur}^{-2.3}$**
- **Time interval : $N \propto t_{int}^{-1.8}$**

$$I \propto \frac{B^2}{t_A} L^3 \propto \frac{B^2}{L/B} L^3 = B^3 L^2$$

$$t_A = L/v_A \propto L/B$$

If B ~ const.

I power-law ⇒ E(~B^2L^3) power-law

t_d (~ t_A) power-law ⇒ L power-law

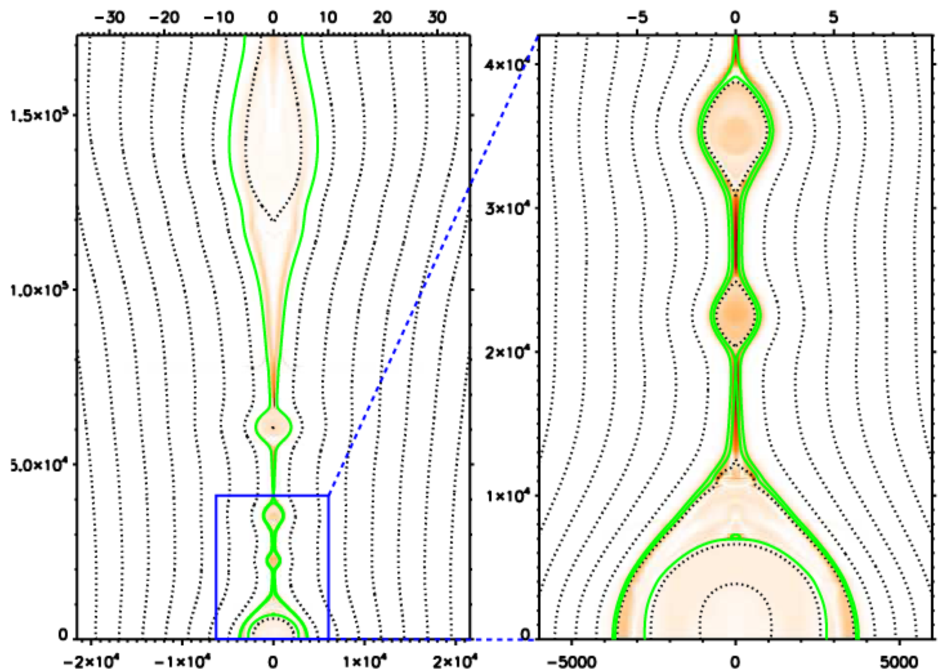

(Barta et al. 2010, presentation on Friday)

- **Kernel intensity (duration) ∝ energy (size) of precipitating particles**

⇒ This indicates the fractal plasmoids or fractal current sheet.

- **Power-law distribution of Time interval ⇒ self-organized criticality**

Power-Law Spectra of 1–2 GHz Narrowband dm-SPIKES : accelerated electrons

(Karlicky et al. 2000)

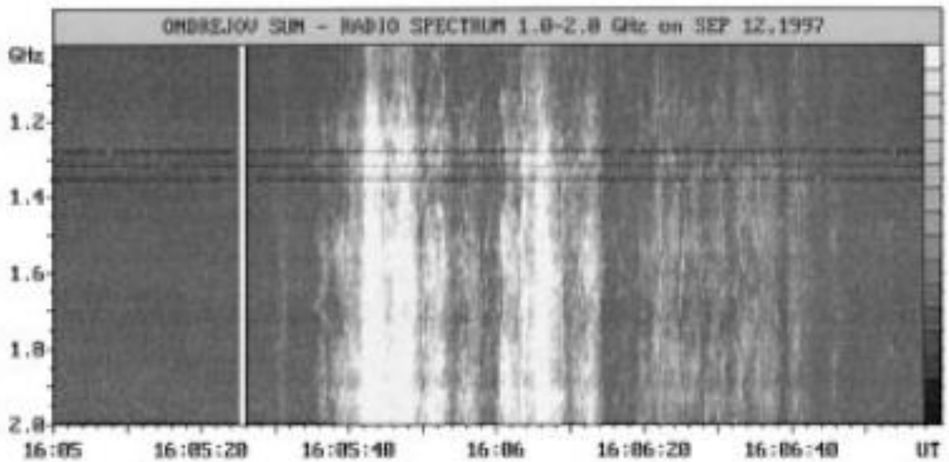

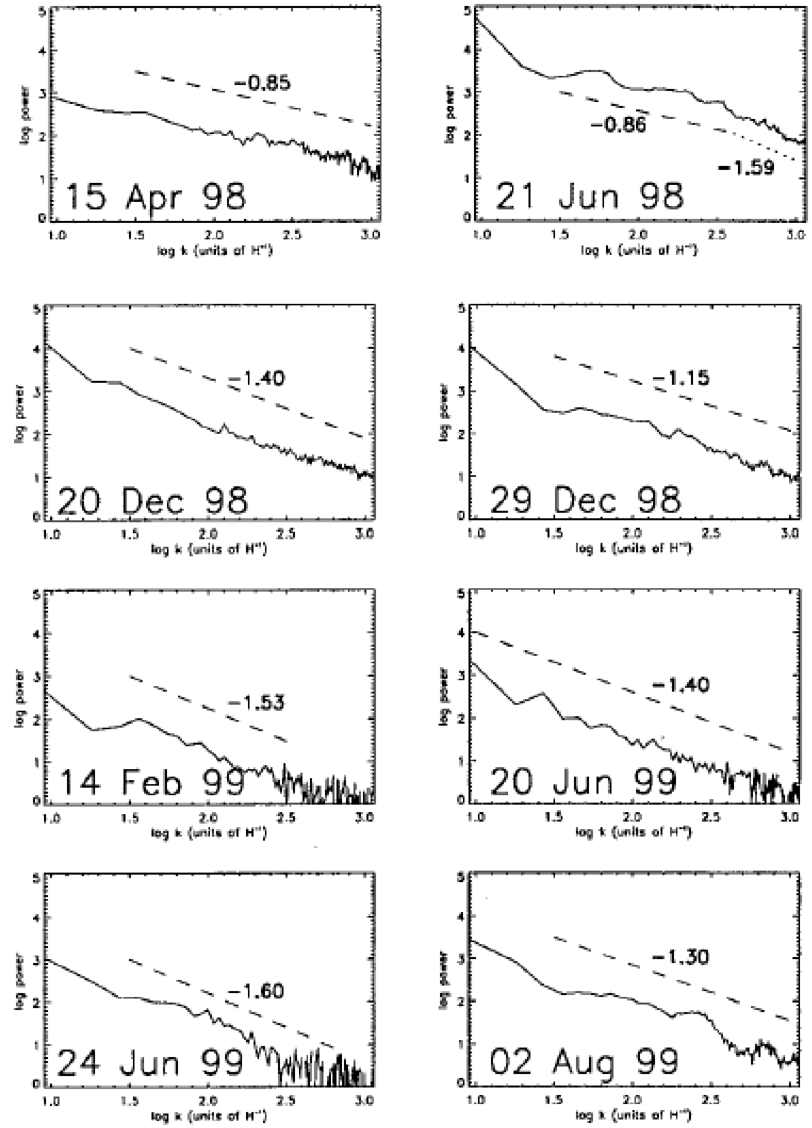

- Fourier spectra of dm-spikes show power-law distribution.
- Power-law index varies depending on event: 0.5-2.85 (index~-5/3)
- This may be evidence of electrons accelerated in MHD cascading waves due to reconnection.

Multiple (fractal) plasmoids collide with fast shocks [Nishizuka & Shibata 2012 submitted, PRL]

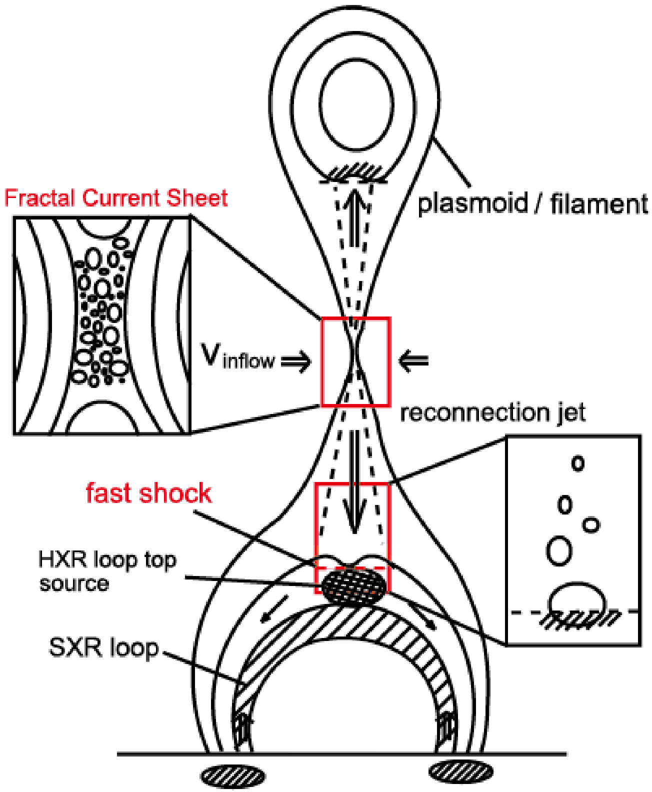

cf) Fermi Acceleration at the fast shock: Somov & Kosugi (1997), Tsuneta & Naito (1998)

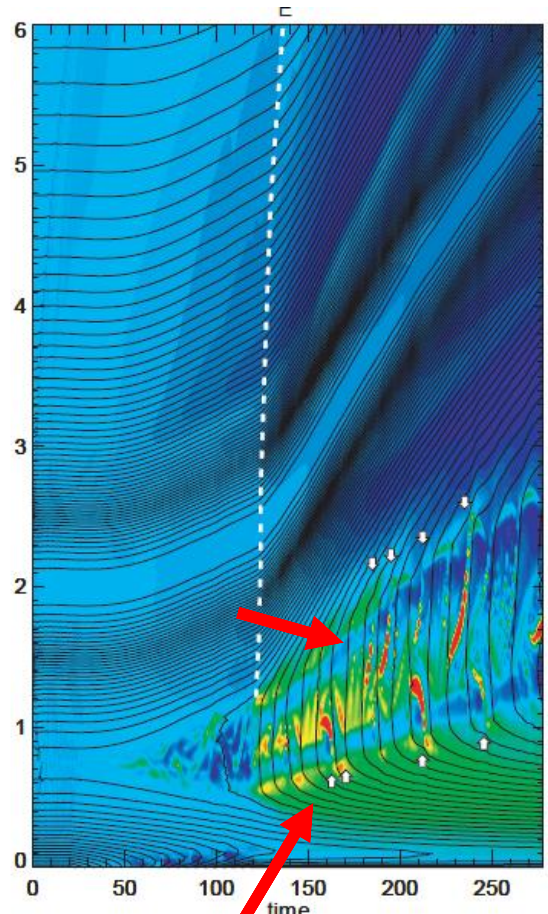

Time slice image of small plasmoid ejections

Shock at the bottom of a large plasmoid

Shock at the loop-top

Plasmoid collide with Fast shock (M_A~1.5)

Multiple (fractal) plasmoids collide with fast shocks [Nishizuka & Shibata 2012 submitted, PRL]

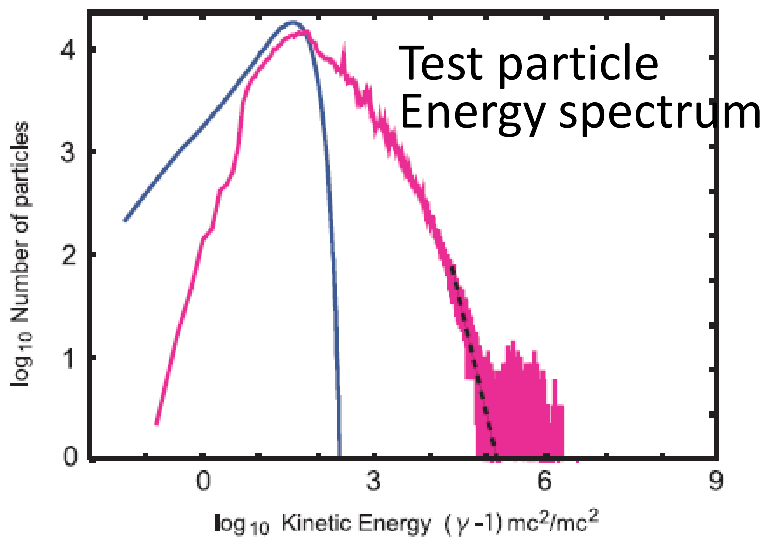

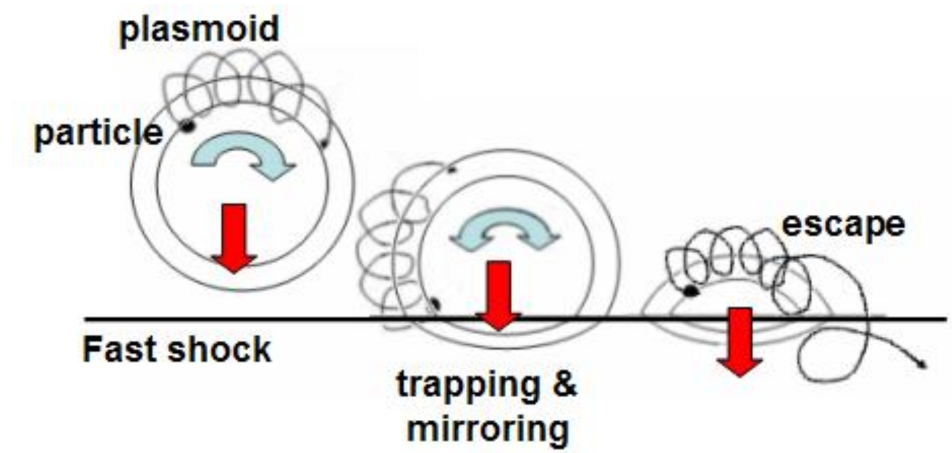

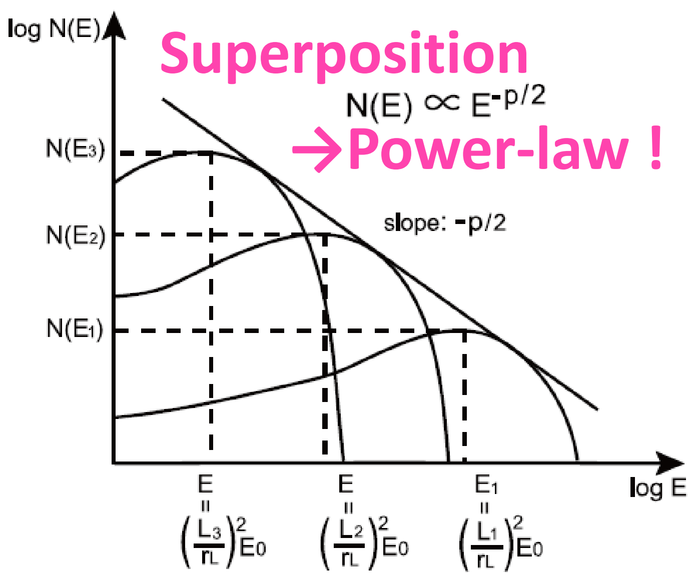

1) Particles are trapped in a plasmoid.
2) Multiple plasmoids collide with fast shock.
3) Particles are reflected due to magnetic mirror effect.
4) Reflection length becomes shorter and shorter.
5) Particles are accelerated by **<u>Fermi process</u>**, until reflection length becomes comparable to ion Larmor radius.

Summary

- We analyzed multi-wavelength observation data (TRACE1600, Hα, RHESSI) of GOES X2.5-class flare on 2004 November 10 with.
- The flare showed several flare kernels inside two-ribbon structure, which were observed in hard X-ray, Hα and C iv emissions. **The Flare kernels are caused by precipitating nonthermal particles**.
- We measured peak intensity, duration and time interval of every 700 kernels in C iv images. As a result, the distributions of peak **intensity**, **duration** and **time interval** follows power-law, whose power-law indexes are 1.5, 2.3, 1.8, respectively.
- The peak intensity, duration and time interval may indicate the **energy**, **size** and **intermittency** of multiple plasmoids in a current sheet. Hence the **power-law distributions of flare kernels may indicate the power-law distributions of multiple plasmoid**, i.e. **fractal current sheet** in a solar flare.
- It is important to know whether and how the fractal (1/f noise) structure is made (and time and spatial variations of power-law index), because it is also related to understanding energy release mechanism.

Huge gap between micro and macro scale in solar flares

- Ion inertial length

$$\ell_{in,ion} = \frac{c}{\omega_{pi}} \approx 300\ cm \left(\frac{n}{10^{10} cm^{-3}} \right)^{-1/2}$$

- Ion Larmor radius

$$r_{Li} = \frac{m_i v c}{eB} \approx 100\, cm \left(\frac{B}{10G} \right)^{-1} \left(\frac{T}{10^6 K} \right)^{1/2}$$

- Mean free path

$$\ell_{mfp} = \frac{1}{n} \left(\frac{kT}{e^2} \right)^2 \approx 10^7 cm \left(\frac{T}{10^6 K} \right)^2 \left(\frac{n}{10^{10} cm^{-3}} \right)^{-1}$$

- Flare size

$$r_{flare} \approx 10^9 cm$$

How many multiple-tearings are necessary to reach microscopic plasma scale?

Fractal Reconnection

[Shibata & Tanuma 2001]

$$\lambda_{n+1} \approx 6\delta_n R_{m^*,n}^{\ \ 1/4} \qquad R_{m^*,n} = \left(\frac{\delta_n V_A}{\eta}\right)$$

$$\delta_n \le \eta^{1/3} V_A^{\ -1/3} \lambda_n^{\ 2/3}$$

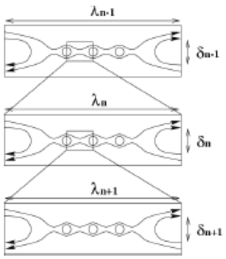

$$\frac{\delta_n}{L} \le 6^{2/3} R_m^{\ -1/6} \left(\frac{\delta_{n-1}}{L}\right)^{5/6}$$

Condition for secondary tearing in Sweet-Paker sheet

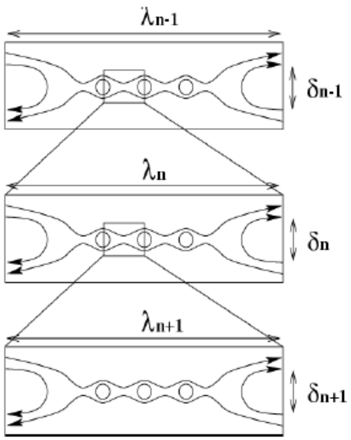

$$t_n \le \lambda_n / V_A$$

$$t_n \approx (t_{dif} t_A)^{1/2} \approx \left(\frac{\delta_n^{\ 3}}{\eta V_A}\right)^{1/2}$$

$$\delta_n \le \eta^{1/3} V_A^{\ -1/3} \lambda_n^{\ 2/3}$$

$$\frac{\delta_n}{L} \le A^{6(1-x)} \left(\frac{\delta_0}{L}\right)^x \qquad A = 6^{2/3} R_m^{\ -1/6}, \quad R_m = L V_A / \eta, \quad x = (5/6)^n$$

$$\delta_n / L < r_{L,ion} / L$$

$$(0.02)^{6(1-(5/6)^n)} (0.1)^{(5/6)^n} < 10^{-7}$$

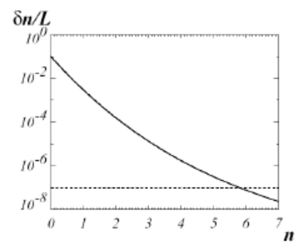

Final solution $\quad n \ge 6$

$$t_n \approx \delta_n^{\ 3/2} (\eta V_A)^{-1/2} = (\delta_n / \delta_0)^{3/2} t_0$$

$$t_0 = \delta_0^{\ 3/2} / (\eta V_A)^{1/2}$$

$$t_n \approx A_0^{\ 6(1-(5/6)^n)} \ t_0$$

$$t_{total} = t_1 + t_2 + t_3 \ .... \ t_n \le t_0 A_0^{\ 3/2} \approx 6 \times 10^{-3} t_0$$

$$t_0 \approx 3 \times 10^4 \sim 10^6 \ \sec \qquad for \ \ \delta_0 \approx 10^7 \sim 10^8 \ cm$$

Plasmoid-induced reconnection

[Shibata & Tanuma 2001]

Analytical model of plasmoid-induced-reconnection: nonlinear instability

Analytical model of pasmoid-induced-reconnection : saturation of nonlinear instability

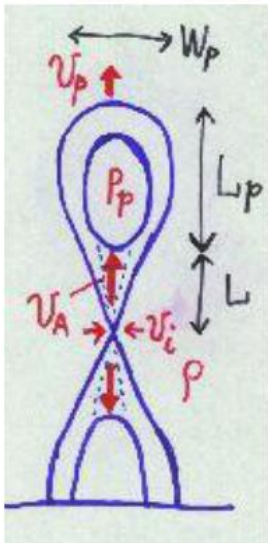

$$\rho_p L_p W_p \frac{dv_p}{dt} = \rho v_i L V_A$$

$$= \rho v_p W_p V_A$$

$$\left(\because v_i = \frac{W_p}{L} v_p \right)$$

Case of Momentum conservation

$$\frac{1}{v_p} \frac{dv_p}{dt} = \omega \equiv \frac{\rho V_A}{\rho_p L_p}$$

$$v_p = v_0 \exp(\omega t)$$

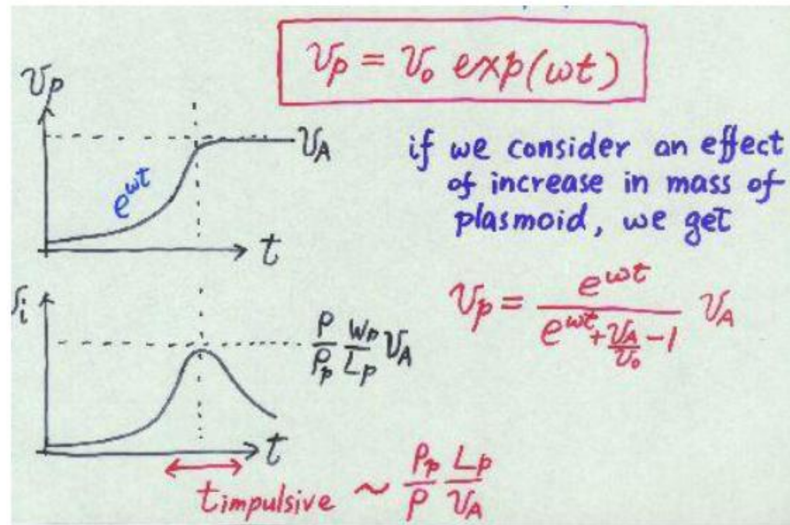

- This can be applied to not only a large plasmoid but also small plasmoids.

Supplement: Initial condition & Perturbation

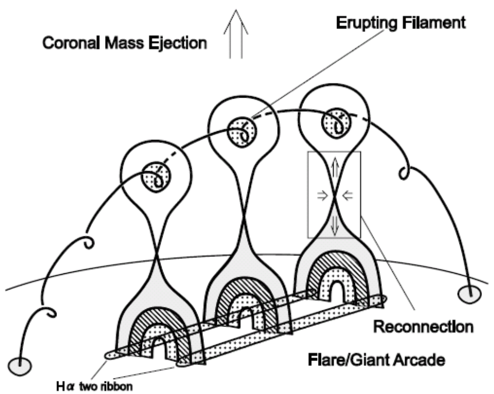

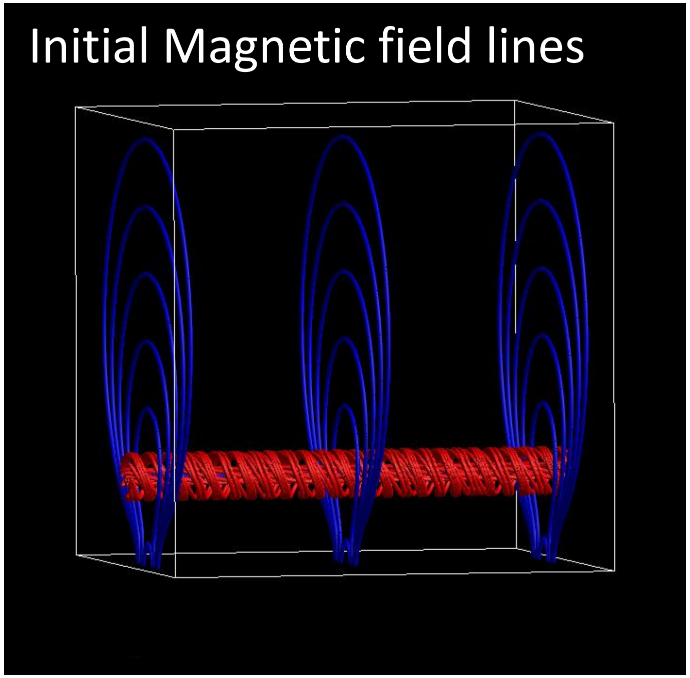

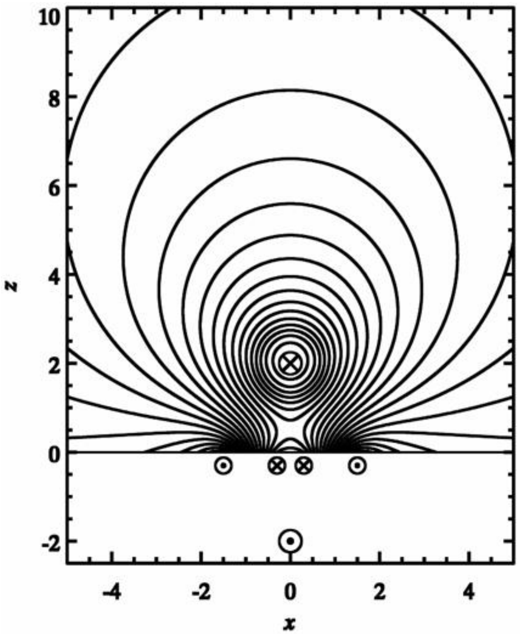

Initial magnetic configuration

- Initially we assumed a flux tube in ``almost'' equilibrium state but unstable, sustained in the corona. No shear motion at the footpoints.
- Slightly lifted up as an initial perturbation (originally by emerging flux).
- Plasma beta β~0.01 at the surface of the flux tube, P_{gas}, T, ρ=const.

Comparison between Type III burst (electron beam) and E-field enhancement in the simulation

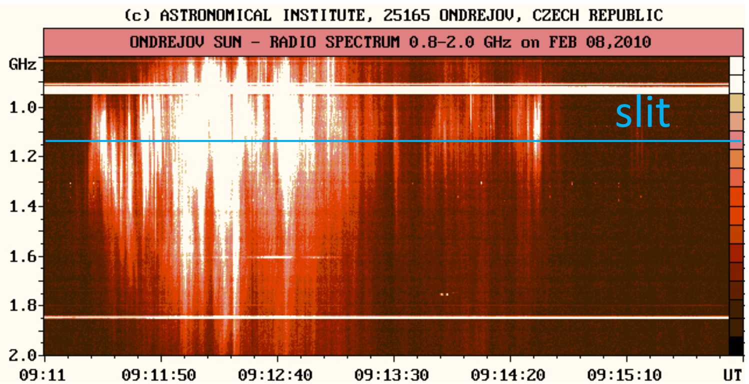

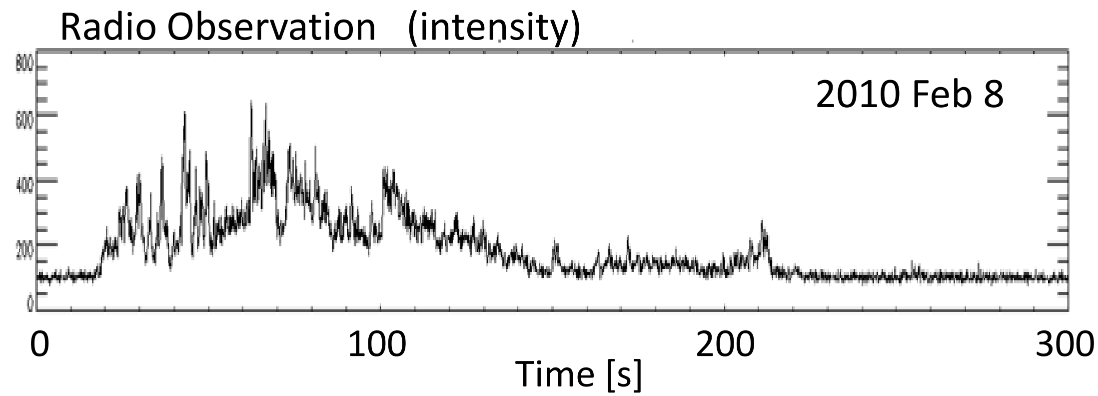

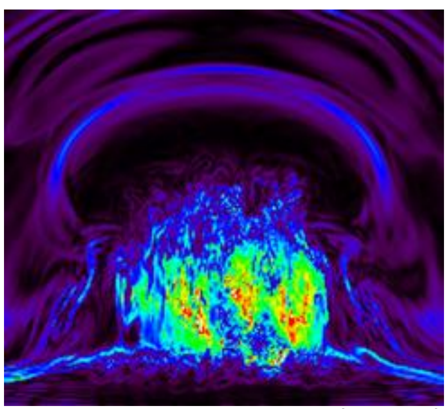

Current density (t=90)

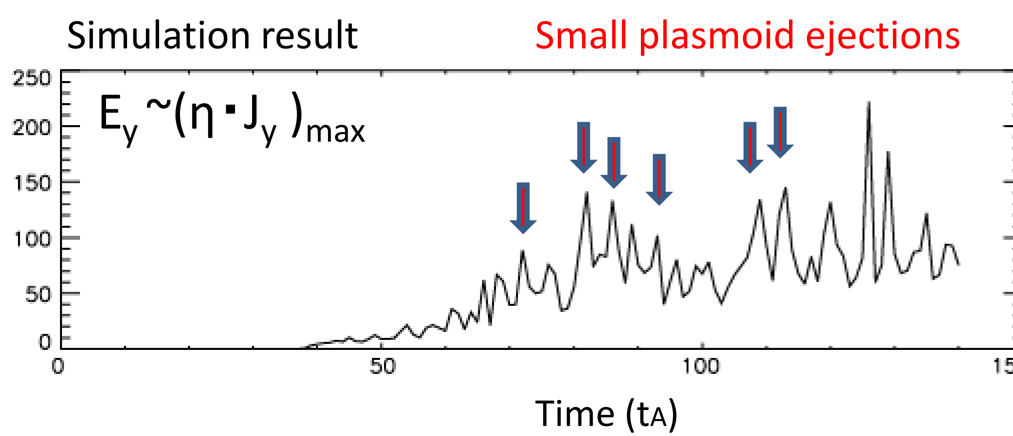

- Simulation show intermittent time variability of E-field enhancement in the turbulent current sheet, as observed in Type III burst. Each of them corresponds to a small plasmoid ejection.